

ONTOGENY AND GEOGRAPHIC VARIATION OF A NEW SPECIES OF THE CORYNEXOCHINE TRILOBITE *ZACANTHOPSIS* (DYERAN, CAMBRIAN)

MELANIE J. HOPKINS¹ AND MARK WEBSTER²

Department of the Geophysical Sciences, University of Chicago, 5734 S. Ellis Ave, Chicago, Illinois 60637 ¹<mjh@uchicago.edu> and
²<mwebster@geosci.uchicago.edu>

ABSTRACT—Assessment of ontogenetic and geographic variation can have substantial influence on species delimitation and thereby on perceived patterns of species-level morphological variation and diversity in space and time. Here we describe the ontogeny and intraspecific variation of the early Cambrian trilobite, *Zacanthopsis palmeri* n. sp., based on silicified material from east-central Nevada, USA. *Zacanthopsis palmeri* is the oldest documented Cambrian corynexochine to shift from possessing a fused rostral-hypostomal plate to a functional hypostomal suture in mature specimens during ontogeny. Six geographically distinct samples of mature *Z. palmeri* from a single silicified limestone bed traceable over tens of kilometers in east-central Nevada permit exploration of geographic variation within this species using geometric morphometric methods. No one sample encompasses all of the shape variation expressed by *Z. palmeri* and several geographically segregated samples show some degree of morphological separation in pairwise comparison. Nonetheless, these samples are not qualitatively or quantitatively different from one another when all samples are taken into account. The degree of variation within *Z. palmeri* is similar in magnitude to the differences between other species in the genus known from much less material.

INTRODUCTION

DISCERNING INTRASPECIFIC variation from interspecific disparity is necessary for species delimitation but nontrivial, particularly if variation exists among spatially segregated localities (geographic variation). Geographic variation has been documented in many extant marine arthropods (e.g., Riska, 1981; France, 1993; Avise, 2000) but to a much lesser extent in the trilobite fossil record (Best, 1961; Cisne et al., 1980a, 1980b, 1982; Hughes, 1994; Webber and Hunda, 2007). In order to measure variation in the fossil record, studies must account for possible non-biological sources of variation, including taphonomic effects, time-averaging, and measurement error, as well as allometric growth (in addition to previous citations, see also Hughes, 1993; Rushton and Hughes, 1996; Webster and Hughes, 1999; Hunda et al., 2006). Because assessment of geographic variation often suffers from uneven sampling of sclerites across localities, many of the papers that describe some degree of intraspecific variation in Cambrian trilobites of Laurentia do not report any spatial segregation of that variation (e.g., Palmer, 1968; Westrop et al., 1996; Lieberman, 1998; Sundberg, 1999, 2004). Certain traits have been interpreted as taxonomically significant in some groups (e.g., granulation in *Dunderbergia* Walcott, 1924 species; Palmer, 1965) but not in others (e.g., potential geographic variation in granulation and pitting in *Saukia*-zone trilobites; Taylor and Halley, 1974). Hughes (1994) found that within-sample variation accounts for most of the variation within and between “species” of *Dikelocephalus* Owen, 1852 and synonymized all previously described species into one (Hughes, 1991, 1994). In contrast, increased sampling of silicified material in some latest Cambrian genera has demonstrated that intraspecific variation is rather low in these faunas; instances where widespread “species” also show between-sample variation have thus been interpreted as species complexes rather than geographic variants (Adrain and Westrop, 2005, 2006; Westrop and Adrain, 2007).

We define a species as “the smallest aggregation of comparable individuals diagnosable by a unique combination

of characters” in the spirit of the phylogenetic species concept of Nixon and Wheeler (1990; see also Wheeler and Meier, 2000). Species may be distinguished using discrete characters or continuously varying characters whose distributions form at least two statistically distinguishable groups.

Zacanthopsis palmeri n. sp. is known only from the upper 2.5 m of the Dyeran (traditional “Lower” Cambrian of Laurentia) of the Pioche district in east-central Nevada (Fig. 1 inset), primarily from silicified beds. Within this 2.5 m stratigraphic interval, most *Zacanthopsis palmeri* material is found in one silicified bed (maximally 30 cm thick) which can be traced for almost 40 km. Although some geographically segregated samples of *Zacanthopsis palmeri* do show some degree of morphological separation in pairwise comparison, they are not qualitatively distinct nor can they be separated into statistically distinguishable groups using morphometric data when all samples are taken into account. By the above criteria, these samples are geographic variants of the same species rather than multiple species.

The nature of the preservation also provides an opportunity to describe in detail the ontogeny of a species of this genus for the first time. Of particular note, the hypostome remains conterminant through ontogeny but shifts from a fused rostral-hypostomal plate to development of a functional hypostomal suture during the meraspid period; other *Zacanthopsis* species that show this characteristic will be documented in a future paper. The only other corynexochine known to have a functional hypostomal suture at maturity is *Fuchouia* (Drumian-Guzhangian, “Middle” Cambrian) for which the ontogeny is currently unknown (Peng et al., 2004; Whittington, 2009). Because *Zacanthopsis* is one of the earlier representatives of this suborder, this feature may have bearing on corynexochine affinities (Whittington, 1988; Fortey, 1990; Chatterton and Speyer, 1997).

Regional setting and materials.—*Zacanthopsis palmeri* occurs predominantly in a single silicified limestone bed that can be traced from the Highland Range southwards into the northern Delamar Mountains (Fig. 1 inset). The bed lies less than 2 meters below the Dyeran-Delamaran boundary (the

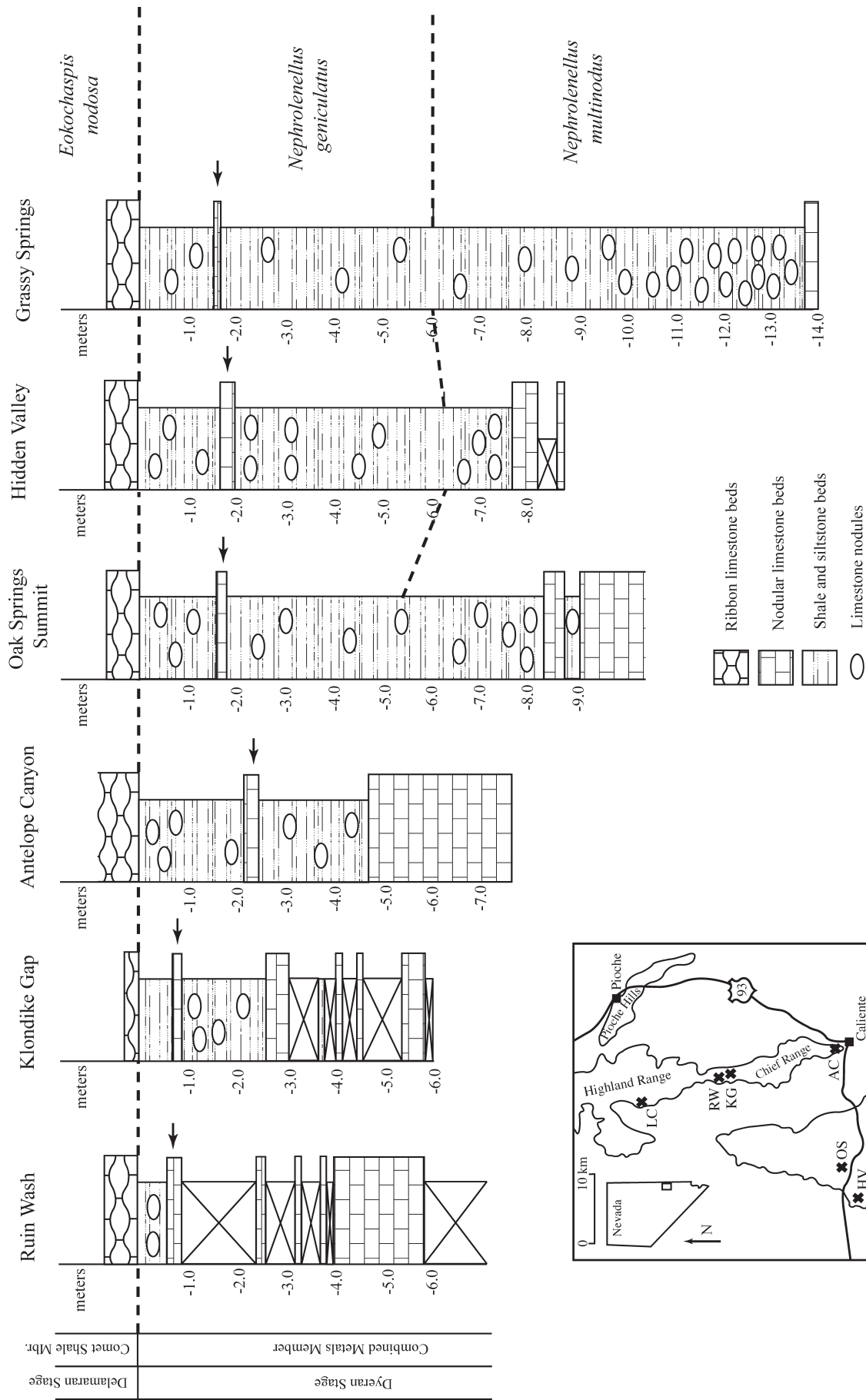


FIGURE 1.—Stratigraphic sections for sampled localities included in analysis of geographic variation. The base of the *Nephrolenellus geniculatus* subzone has not yet been identified at Klondike Gap or Antelope Canyon; at Ruin Wash, the base of this biozone is located between -1.0 and -5.0 m. Based on Palmer (1998), Webster (2007a, 2007b), Webster et al. (2008); and unpublished field notes. Inset: Map of sample localities, east-central Nevada, USA. AC = Antelope Canyon; GS = Grassy Springs; HV = Hidden Valley; KG = Klondike Gap; LC = Log Cabin Mine and One Wheel Canyon; OS = Oak Springs; RW = Ruin Wash. Modified from Sundberg and McCollum (2000).

traditional “Lower-Middle Cambrian” boundary of Laurentia in the upper part of the Combined Metals Member of the Pioche Formation (Sundberg and McCollum, 2000). The Pioche Formation is a sequence of alternating siliciclastics and carbonates that range through the upper Dyeran and into the Delamaran (Merriam, 1964; Palmer, 1971; Eddy and McCollum, 1998; Palmer, 1998; Sundberg and McCollum, 2000). The *Z. palmeri* bed is the highest Dyeran nodular limestone bed in a section of interbedded shales and nodular limestone beds. Karsted calcareous sandstone and oncolitic limestones below the section of nodular limestone beds, and ribbon limestones above the section of nodular limestone beds (Fig. 1, see also Sundberg and McCollum, 2000), indicate that water depth was increasing as these sediments were deposited (Webster, 2007b). This stratigraphy is consistent across all localities where *Z. palmeri* is present. Using the highest biostratigraphic resolution available (Webster, 2003), the sampled bed consistently falls within the uppermost portion of the uppermost trilobite subzone of the Dyeran, and is no more than 30 cm thick at all localities (Fig. 1). Thus, while it is unclear how much absolute time is represented by this bed, samples from this bed are deemed to be consistently time-averaged and any diachroneity across localities is negligible.

The limestone bed was sampled from six localities between 1993 and 2005: Ruin Wash (see Figs. 2, 6.25–39, 6.41 for selection of specimens), Klondike Gap (Figs. 3, 6.40, 6.42–51), Antelope Canyon (Fig. 4.1–24), Oak Springs Summit (Fig. 5.1–11), Hidden Valley (Fig. 5.12–21), and Grassy Spring (Fig. 4.29–32). Stratigraphic sections for these localities have previously been published for Ruin Wash (Palmer, 1998; Webster et al., 2008), Klondike Gap (Webster, 2007b), Antelope Canyon (Sundberg and McCollum, 2000), Oak Springs Summit (Palmer, 1998), Hidden Valley (Palmer, 1998; Sundberg and McCollum, 2000), and Grassy Spring (Palmer, 1998). Additional studies describing material from this bed include Sundberg and McCollum (1997), Webster and Hughes (1999), Webster et al. (2001), Sundberg (2004), and Webster and Zelditch (2005). Smith (1995, 1998a, b) described older *Zacanthopsis* material from some of these localities.

Olenelloid and ptychoparioid trilobites serve as biostratigraphic indicators for correlation between the sections (Fig. 1). Several species of brachiopod, and rarely pelagiellids, the trilobite *Bathynotus*, and oryctocephalid trilobites are also preserved in this bed. The relative and absolute abundance of *Zacanthopsis palmeri* varies across these localities, and large sample sizes of complete cranidia were not available from Oak Springs Summit (N = 6) and Grassy Spring (N = 2). *Zacanthopsis palmeri* is also found in limestones at Log Cabin Mine (Fig. 4.25–28) and One Wheel Canyon in the northern Highland Range. While these limestones are both within a couple meters of the Dyeran-Delamaran boundary, these samples could not be correlated with other localities to the same resolution and were not included in the analysis of geographic variation.

Although the quality of preservation of exoskeletal features varies among silicified specimens of *Z. palmeri*, the specimens

have not suffered taphonomic deformation (i.e., compaction or shearing). Lack of obvious size sorting (see below) and the presence of delicate features such as axial spines on sclerites and rare articulated specimens indicate that the fossil material was not appreciably transported. The vast majority of specimens are disarticulated, however; therefore variation is assessed separately within cranidia and pygidia. Because apparent intraspecific variation can be inflated by ontogenetic variation (variation in morphology due to allometric growth), the ontogenetic rate of shape change in each sclerite relative to size was used to identify morphologically mature specimens. Variation due to allometric growth in mature specimens was then removed using multiple regression of shape variables on size (see “Choice of specimens for analysis” and “Removal of variation due to allometry” under Geographic Variation).

Specimen preparation.—Specimens were removed from the limestone bed by dissolution of the carbonate matrix in dilute acetic acid. The specimens were then picked from the remaining insoluble residue, blackened with India ink, and whitened with ammonium chloride prior to photography. Cranidia were oriented for photography in dorsal view with the lateral edges of the anterior and posterior branches of the facial suture horizontal. Because the specimens are so small and the palpebral lobe is arched in lateral view, these criteria facilitate consistent orientation. In this orientation the chord of the palpebral lobe is generally horizontal as recommended by Shaw (1957). Pygidia were oriented in dorsal view with the inner pleural field horizontal and the articulating and ring furrows vertical. This is not consistent with Shaw (1957), but is necessary for viewing posterior features, such as pygidial spines, in dorsal view.

SYSTEMATIC PALEONTOLOGY

Terminology.—Morphological terminology follows that of Whittington and Kelly (1997) and Palmer (1998). FMNH: Field Museum of Natural History (Chicago, IL); GSC: Geological Society of Canada; ICS: Institute for Cambrian Studies (University of Chicago); UCR: University of California, Riverside; USNM: U.S. National Museum (Smithsonian).

Order CORYNEXOCHIDA Kobayashi, 1935
Suborder CORYNEXOCHINA Kobayashi, 1935
Family ZACANTHOIDIDAE Swinerton, 1915
Genus ZACANTHOPSIS Resser, 1938
ZACANTHOPSIS PALMERI n. sp.
Figures 2–7, 10–11

Diagnosis.—*Zacanthopsis* with hemicylindrical glabella, very slightly expanding forward. Palpebral lobes over two thirds the length of the glabella, well defined, strongly curved, extending laterally beyond frontal area and posterior wings. Ocular ridges as long as width of glabella, well defined, of uniform width, contacting glabella at posterior third of LA. Posterior wings narrow (tr.). Pygidium with large semicircular axial lobe; two axial furrows behind articulating furrow; four pairs of short, triangular pleural spines.

Description (mature morphology: 1.6–5.8 mm in cephalic length; 0.5–1.9 mm in total pygidial length).—Cranidium

Figure 2—Morphologically mature cranidia and librigena of *Zacanthopsis palmeri* n. sp. 1, 5, 14, 19, librigena, dorsal, ventral, anterior, and lateral views, FMNH PE58158, $\times 7$; 2, 18, 27, librigena, dorsal, anterior, and oblique views, FMNH PE58159, $\times 7$; 3, 7, 8, 12, 13, cranidium, dorsal, lateral, ventral, posterior, and anterior views, FMNH PE58141, $\times 7$; 4, 9, 10, 16, 17, cranidium, dorsal, ventral, lateral, posterior, and anterior views, FMNH PE58144, $\times 12$; 6, librigena, dorsal view, FMNH PE58160, $\times 15$; 11, 25, cranidium, lateral and oblique views, FMNH PE58143, $\times 10$; 15, 20, 21, 28, 29, cranidium, lateral, posterior, anterior, dorsal, and ventral views, FMNH PE58147, $\times 15$; 22, 26, cranidium, dorsal and oblique views, FMNH PE58142, $\times 7$; 23, cranidium, dorsal view, FMNH PE58150, $\times 20$; 24, cranidium, dorsal view, FMNH PE58148, $\times 15$; 30, cranidium, dorsal view, FMNH PE58149, $\times 17$; 31, 33, cranidium, dorsal and lateral views, FMNH PE58145, $\times 10$; 32, cranidium, dorsal view, FMNH PE58146, $\times 12$. All from Ruin Wash.

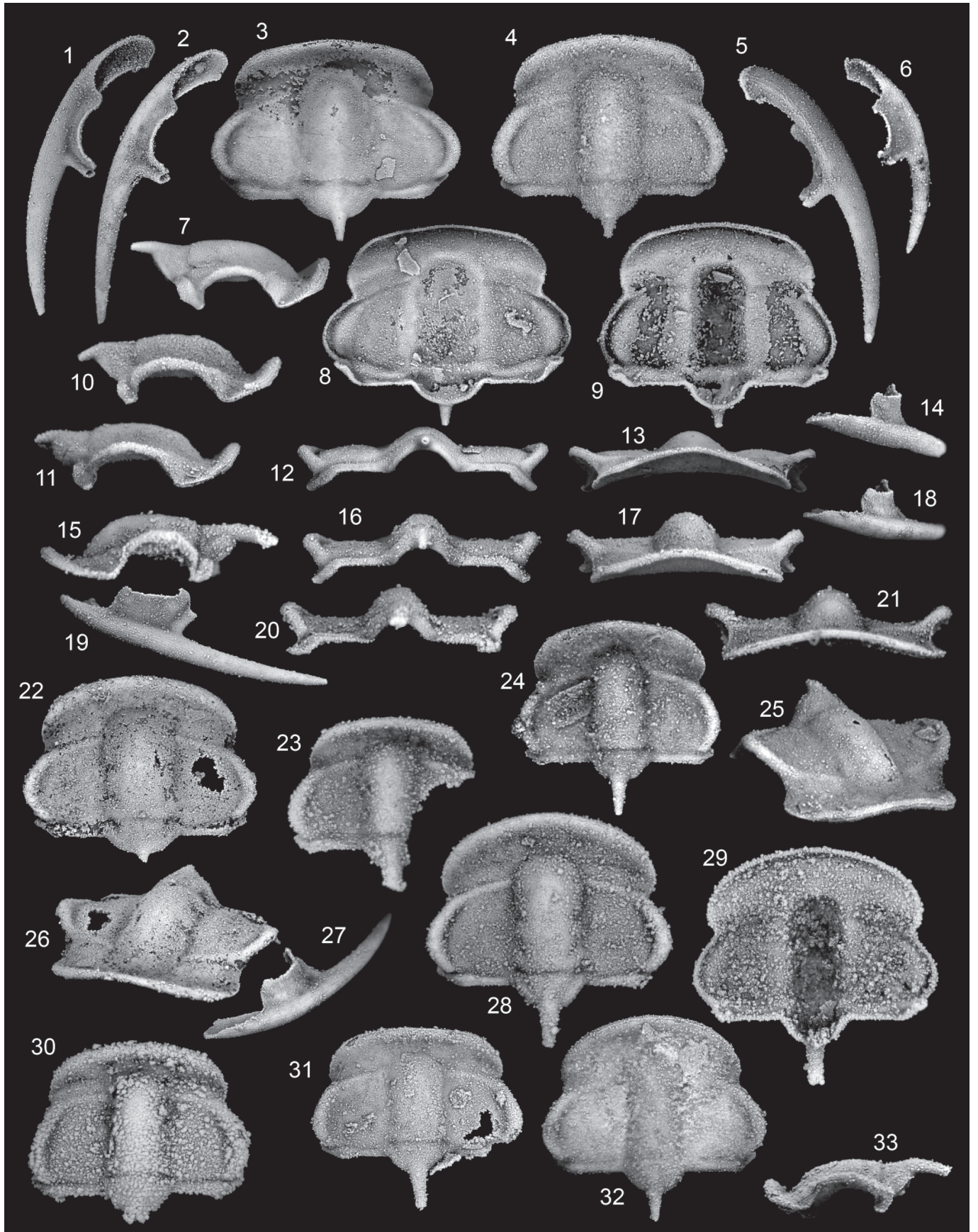




FIGURE 3—Morphologically mature cranidia of *Zacanthopsis palmeri* n. sp. 1, 5, 9, 13, 20, cranidium, dorsal, ventral, anterior, posterior and lateral views, FMNH PE58174 (holotype), $\times 10$; 2, 6, 10, 14, 19, cranidium, dorsal, ventral, anterior, posterior and lateral views, FMNH PE58175, $\times 10$; 3, 8, 12, 16, 17, cranidium, dorsal, ventral, anterior, posterior and lateral views, FMNH PE58177, $\times 12$; 4, cranidium, dorsal view, FMNH PE58179, $\times 15$; 7, cranidium, dorsal view, FMNH PE58178, $\times 15$; 11, 15, 18, cranidium, anterior, posterior, and dorsal views, FMNH PE58176, $\times 12$. All from Klondike Gap.

subquadrate in outline. Anterior border slightly narrower (sag.) than width (tr.) of palpebral lobes; gentle anterior arch; doublure narrower than anterior border. Very shallow anterior border furrow; sharp upturn in preglabellar field, sharpest laterally. Glabella expands slightly anteriorly, narrowest at S2. LA rounded anteriorly; preglabellar furrow usually shallower than axial furrows. Dorsal glabellar surface smoothly arched (long.) from occipital furrow to preglabellar field; slope sometimes increases in strength anteriorly. Frontal area strongly concave; anterior arch higher than interocular area but lower than dorsal surface of glabella. Dorsal surface of glabella higher than palpebral lobes with rare exception (Fig. 3.10, 3.14). Interocular areas generally horizontal; occasionally sloping down adaxially (Fig. 3.10, 3.14) or slightly arched (Figs. 2.12, 4.10). Facial sutures opisthoparian; anterior branch diverges from ocular ridges before curving adaxially to merge smoothly with anterior margin. Four glabellar furrows, less well defined anteriorly: S1 oriented

postero-adaxially, SO and S2 transverse, S3 and S4 oriented antero-adaxially (Figs. 2.28, 5.1–2); all deepest abaxially, only SO crosses sagittal axis. Posterior margin of LO curves posteriorly. Doublure under LO curves dorsally, extends anteriorly almost to SO (Figs. 2.8, 5.18). Occipital spine shorter than width (sag.) of LO with rare exception (Fig. 5.15), extending posteriorly either horizontally (Figs. 2.7, 4.5), or dipping slightly ventrally (Figs. 2.10, 4.6). Ocular ridges as long as width of glabella, well defined, distinctly narrower than palpebral lobes, of uniform width, terminate at posterior third of LA, extend postero-laterally from glabella at 80° relative to sagittal axis. Palpebral lobes at least two thirds length of glabella, arcuate; oriented obliquely to sagittal axis, anterior ends closer to one another than posterior ends, widest (tr.) at lateralmost extent with tapering anterior and posterior ends; curvature strongest at lateralmost extent. Palpebral lobe extends to posterior border furrow, sometimes to occipital furrow in lateral view (compare Fig. 2.7

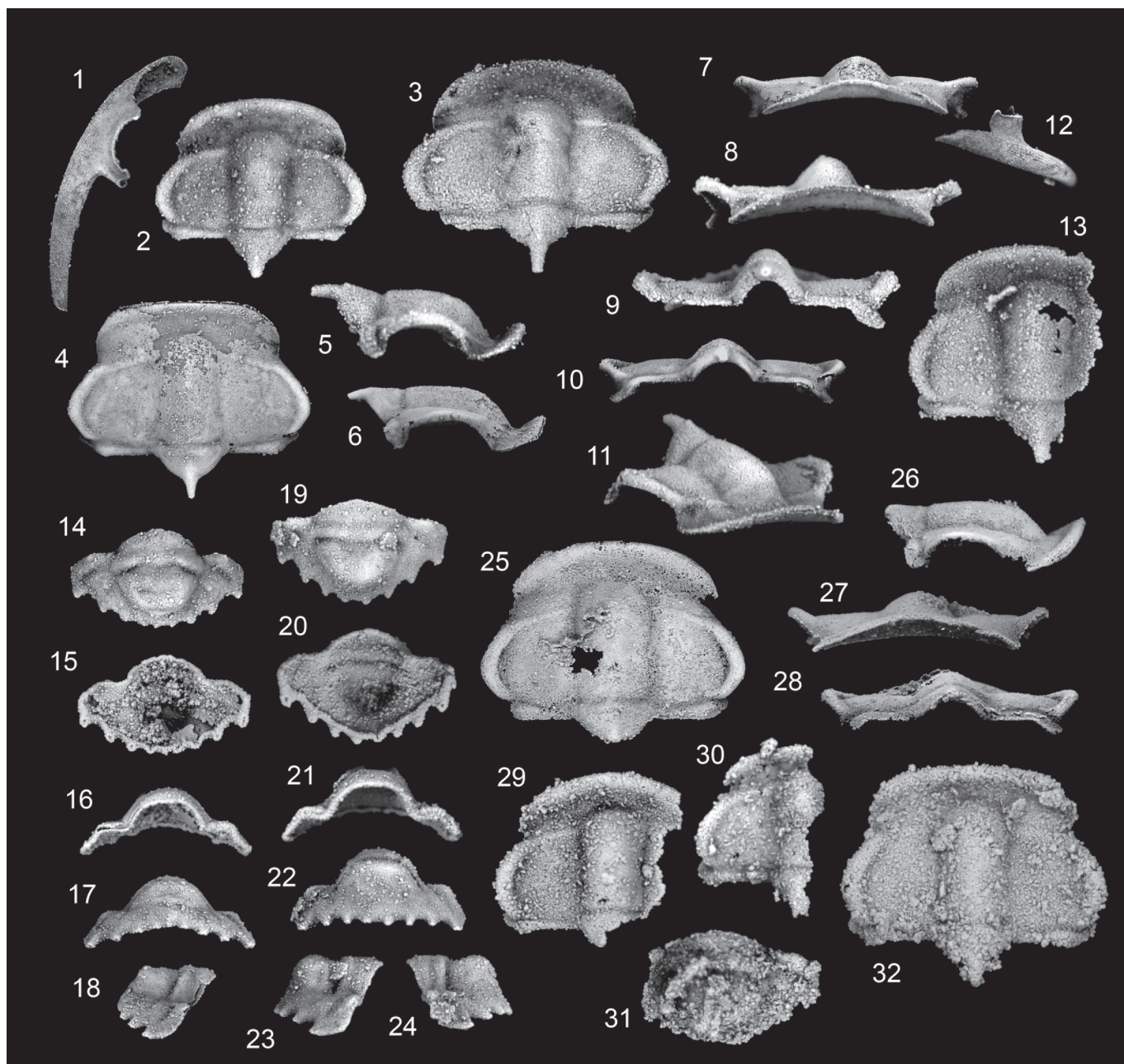


FIGURE 4—Morphologically mature cranidia, librigena and pygidia of *Zacanthopsis palmeri* n. sp. 1, 12, librigena, dorsal and anterior views, FMNH PE58213, $\times 12$; 2, cranidium, dorsal view, FMNH PE58203, $\times 15$; 3, 5, 8, 9, 11, cranidium, dorsal, lateral, anterior, posterior, and oblique views, FMNH PE58202, $\times 15$; 4, 6, 7, 10, cranidium, dorsal, lateral, anterior and posterior views, FMNH PE58201, $\times 7$; 13, cranidium, dorsal view, FMNH PE58204, $\times 17$; 14–18, pygidium, dorsal, ventral, anterior, posterior and lateral views, FMNH PE58216, $\times 10$; 19–24, pygidium, dorsal, ventral, anterior, posterior, and right and left lateral views, FMNH PE58217, $\times 15$; 25–28, cranidium, dorsal, lateral, anterior, and posterior views, FMNH PE58218, $\times 7$; 29, cranidium, dorsal view, FMNH PE58220 $\times 15$; 30, cranidium, dorsal view, FMNH PE58221, $\times 20$; 31, pygidium, dorsal view, FMNH PE58222, $\times 15$; 32, cranidium, dorsal view, FMNH PE58219, $\times 15$. 1–24 are from Antelope Canyon, 25–28 from Log Cabin Mine, and 29–32 from Grassy Spring.

with 2.10 and 2.11), extending laterally beyond posterior wing. Palpebral furrow wider than any other furrows. Posterior border straight (tr.), extends across posterior wing, narrower than but as deep as palpebral furrow. Posterior wing curves ventrally and anteriorly at fulcrum, tapers laterally; doublure along posterior wing widens distally from fulcrum (Fig. 2.8–9). Very fine granulation on interocular areas, frontal area posterior of anterior border, and ocular ridge visible on at least some specimens (Fig. 5.2).

Librigena much narrower (tr.) than interocular area, defined by very shallow border furrow (Fig. 2.1) that may

appear only as break in slope (Fig. 2.2, 2.6). Ocular platform narrower than anterior and lateral border. Doublure as wide as anterior border. Genal spine at least as long as pre-occipital cranidial length; as wide as doublure at base, tapers to point; hollow, circular in cross-section; extends posteriorly following curvature of anterior border and doublure. Tall eye socle (Fig. 2.14, 2.18, 2.19, 2.27). Terrace lines on outer margin and genal spine.

Hypostome ovate with bulbous anterior lobe. Anterior wings triangular, extend dorso-laterally (Fig. 7.1, 7.4, 7.8). Posterior wings longer than anterior wings with bluntly

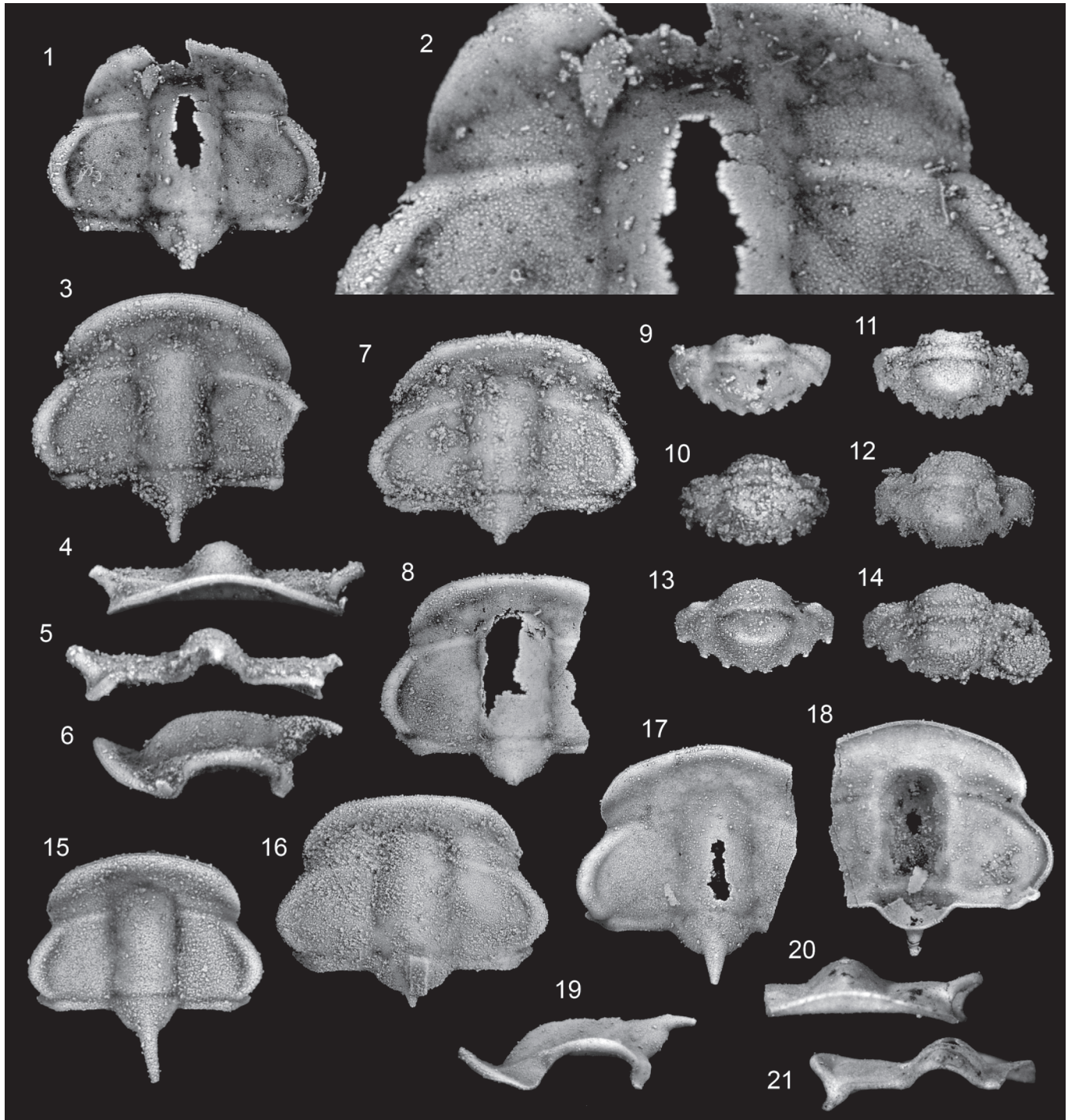


FIGURE 5—Morphologically mature crania and pygidia of *Zacanthopsis palmeri* n. sp. 1, 2, cranium, dorsal view and magnified partial view showing granular ornament, FMNH PE58226, $\times 15$, $\times 40$; 3–6, cranium, dorsal, anterior, posterior, and lateral views, FMNH PE58225, $\times 15$; 7, cranium, dorsal view, FMNH PE58223, $\times 10$; 8, cranium, dorsal view, FMNH PE58224, $\times 10$; 9, pygidium, dorsal view, FMNH PE58232, $\times 20$; 10, pygidium, dorsal view, FMNH PE58233, $\times 20$; 11, pygidium, dorsal view, FMNH PE58231, $\times 15$; 12, pygidium, dorsal view, FMNH PE58241, $\times 10$; 13, pygidium, dorsal view, FMNH PE58240, $\times 10$; 14, pygidium, dorsal view, FMNH PE58242, $\times 12$; 15, cranium, dorsal view, FMNH PE58236, $\times 15$; 16, cranium, dorsal view, FMNH PE58234, $\times 7$; 17–21, cranium, dorsal, ventral, lateral, anterior, and posterior views, FMNH PE58235, $\times 10$. 1–11 from Oak Springs Summit and 12–21 from Hidden Valley.

rounded tips, extend directly dorsally; not visible in ventral view (Fig. 7.1–3). Posterior wings narrower than anterior wings, distinct from marginal border of hypostomal body. Posterior body well defined by arcuate transverse furrow, no wider (sag.) than anterior wings. Posterior margin more strongly curved than hypostomal suture. Border very narrow,

well defined. On largest specimens, large maculae prominent on posterior part of anterior body (Fig. 7.1, 7.4). No ornamentation.

Rostral plate hemicylindrical, broadly curved at anterior margin (rostral suture) (Fig. 7.18–26). Body of plate twice as wide (tr.) as long (sag.). Anterior wings long, narrow;

posterior wings shorter than anterior wings with wide blunt ends. Lateral edges (connective sutures) strongly convex adaxially. Terrace lines present across ventral surface (Fig. 7.21–22).

Each thoracic segment narrow, with length (tr.) to width (exsag.) ratio of each pleura ranging from 1.5 to 3; of uniform width (exsag.). Articulating ring well defined by moderately wide (exsag.) furrow, widest medially. Pleural furrow triangular, as wide as axial ring adaxially, tapers distally to point, extends almost to postero-lateral edge. Pleura curves ventrally at fulcrum, angle of curvature varies from 40° to 50° across segments (Fig. 6.1–24). Sentate pleural spine on all segments. Macroaxial spine present on at least one segment with short (tr.) pleura and strong fulcrum. Macroaxial spine up to ten times as long as segment width (sag.) (Fig. 6.7, 6.13), upsloping at around 45° angle from pleura, terrace lines present. Upsloping axial spines present on all other segments but shorter than segment width (sag.) (Fig. 6.14–18).

Pygidium small, subtriangular, with semicircular axial lobe. Two axial furrows behind prominent articulating furrow; anteriormost ring furrow as wide (sag.) medially as first axial ring, narrows distally, deepest anteriorly; posteriormost ring furrow defined by shallow indentation in middle of axis, rarely extends to axial furrow (Figs. 4.14–18, 6.25–29). Articulating furrow and anteriormost ring furrow visible on the ventral surface as prominent ridges. Axial furrow represented by change in slope between axial rings and pleural field. Anterior margin curves ventrally midway along pleural field at approximately 45° relative to sagittal axis. Two pleural furrows; posteriormost often poorly defined. Pleural furrows extend back from anterior border at about 45° relative to sagittal axis; extend to middle of the base of triangular spine (Fig. 6.41). Four pairs of short, blunt, triangular pleural spines; decrease in size posteriorly. Lateral edge of anteriormost spine meets anterior margin at approximately 80°. Border furrow absent. Doublure on posterior margin no wider (exsag.) than length of pleural spines (Figs. 4.20, 6.26, 6.36).

Etymology.—Named for A. R. Palmer, who has conducted much work on Cambrian trilobites of the Great Basin.

Types.—Holotype, cranidium, FMNH PE58174, and paratypes, FMNH PE58187, FMNH PE58190–193, FMNH PE58195, from the Combined Metals Member, Pioche Formation (late Dyeran), Klondike Gap, Chief Range, Lincoln County, eastern Nevada. Paratypes, FMNH PE58144, FMNH PE58166, FMNH PE58167, FMNH PE58158, FMNH PE58164, from the Combined Metals Member, Pioche Formation (late Dyeran), Ruin Wash, Chief Range, Lincoln County, eastern Nevada. Paratype, FMNH PE58216, from the Combined Metals Member, Pioche Formation (late Dyeran), Antelope Canyon, Chief Range, Lincoln County, eastern Nevada.

Material examined and occurrence.—NEVADA: *Highland Range, Lincoln County:* ICS-1234 (Log Cabin Mine section, Combined Metals Member of the Pioche Formation, 20 cm below top Dyeran). ICS-1077 (One Wheel Canyon section, Combined Metals Member of the Pioche Formation, 0.9 m below top Dyeran). *Delamar Mountains, Lincoln County:* ICS-1280 and ICS-10252 (Grassy Springs section, 1.5 m below the top Dyeran). ICS-1287 and ICS-10101 (Oak Springs Summit section, Combined Metals Member of the Pioche Formation, carbonate nodules 1.6 m below the top Dyeran). *Chief Range, Lincoln County:* ICS-1233 and ICS-10020 (Antelope Canyon section, Combined Metals Member of the Pioche Formation, 2.05–2.33 m below top Dyeran). ICS-1048 and ICS-10010

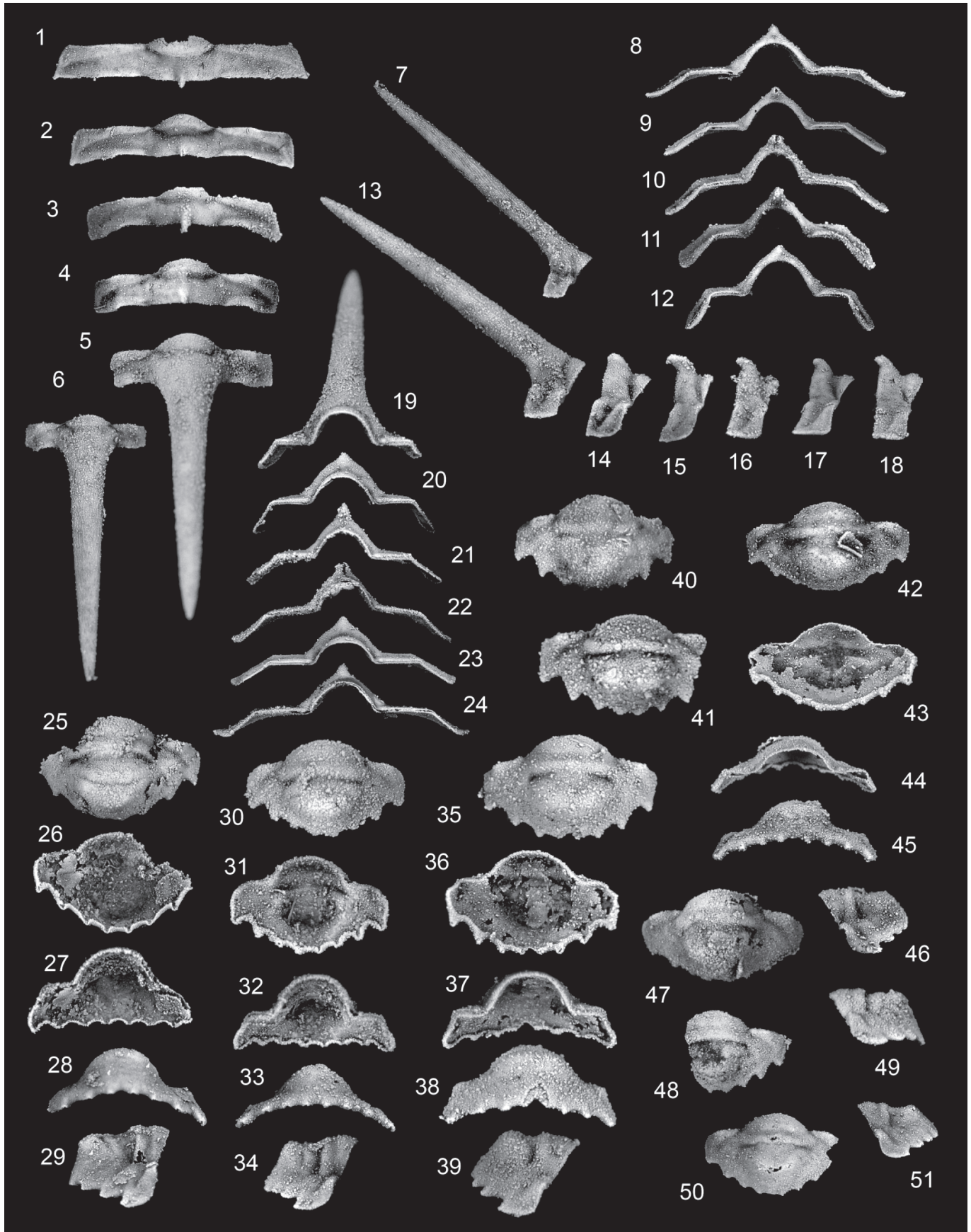
(Ruin Wash section, Combined Metals Member of the Pioche Formation, 24.3–24.54 m above erosion surface at base of Combined Metals Member). ICS-1103 and UCR 10097 (Klondike Gap section, Combined Metals Member of the Pioche Formation, 0.65–0.75 m below top Dyeran). *Burnt Springs Range, Lincoln County:* ICS-1173 and UCR 9963 (Hidden Valley section, Combined Metals Member of the Pioche Formation, carbonate nodules 1.8 m below the top Dyeran). All material except that from One Wheel Canyon is silicified.

Discussion.—Silicified *Zacanthopsis palmeri* specimens permit a more nearly complete description of the morphology and ontogeny of the species than is known for other species of the genus. Two articulated specimens of *Zacanthopsis* are known from shales at Ruin Wash and Grassy Spring but cranidial features on both specimens are not sufficiently well preserved to permit species identification. Newly collected silicified material of *Z. levis* was also examined for comparative purposes (see also Smith, 1995). A full revision of the genus will be presented elsewhere.

The *Zacanthopsis palmeri* cranidium differs from that of *Z. levis* (Walcott, 1886) by being distinctly narrower (tr.) between the anterior branches of the facial sutures than between the palpebral lobes (Fig. 8.1). *Zacanthopsis contractus* Palmer, 1964 and *Z. expansa* Fritz, 1991 also share this distinction from *Z. levis* (Fig. 8.3, 8.7–8). *Zacanthopsis palmeri* differs from *Z. contractus* by having a more gently anteriorly expanding glabella and longer ocular lobes (with the exception of *Z. contractus* specimen GSC 27416, previously described as *Z. stribuccus* Fritz, 1972, Fig. 8.6). *Zacanthopsis palmeri* differs from *Z. expansa* by lacking any increase in ocular ridge width towards the palpebral lobes and by having longer ocular ridges (Fig. 8.7–8). The pygidium of *Z. palmeri* differs from that of *Z. expansa* and *Z. levis* by having fewer axial furrows defined behind the articulating furrow despite having the same number of pleural spines (Fig. 8.4–5). The pygidium for *Z. contractus* is not known.

Unlike most other corynexochines, the hypostome and rostral plate were not fused in mature individuals of *Zacanthopsis palmeri*. Cranidia may be grouped with librigena of similar sutural morphology and size to estimate the gap size between the librigena where the rostral plate would fit. Rostral plates of the appropriate length (tr.) were wide (sag.) enough to reach the preglabellar furrow, indicating a conterminant hypostomal position (Fortey, 1990) with a functional hypostomal suture. The hypostomal suture must end where the posterior wing of the rostral plate begins (this is represented as a kink in the anterior border of the hypostome in ventral view). Using this functional constraint, the size of the associated hypostome can be estimated; the posterior margin of the hypostome likely lay beneath L2. Although the posterior wings (Fig. 7.2–3) may have been long enough to brace the hypostome against the ventral side of the cranidium, there are no definitive apodemal pits along the axial furrow indicating attachment sites of the wings.

Because of the tall eye socle, the visual surface must have been quite narrow vertically (see Fig. 2.26–27). If the visual surface was horizontal in life, the genal spines would have sloped downwards posteriorly (Fig. 2.19), dipping below the lateral tips of the thoracic segments. It is possible that the genal spines lay about parallel to the ground and that the visual surface sloped anteriorly, as has been argued for other trilobites (e.g., *Dikelocephalus*: Hughes, 1993). In this orientation, the field of vision in the vertical plane would have been greater than if the visual surface were horizontal.



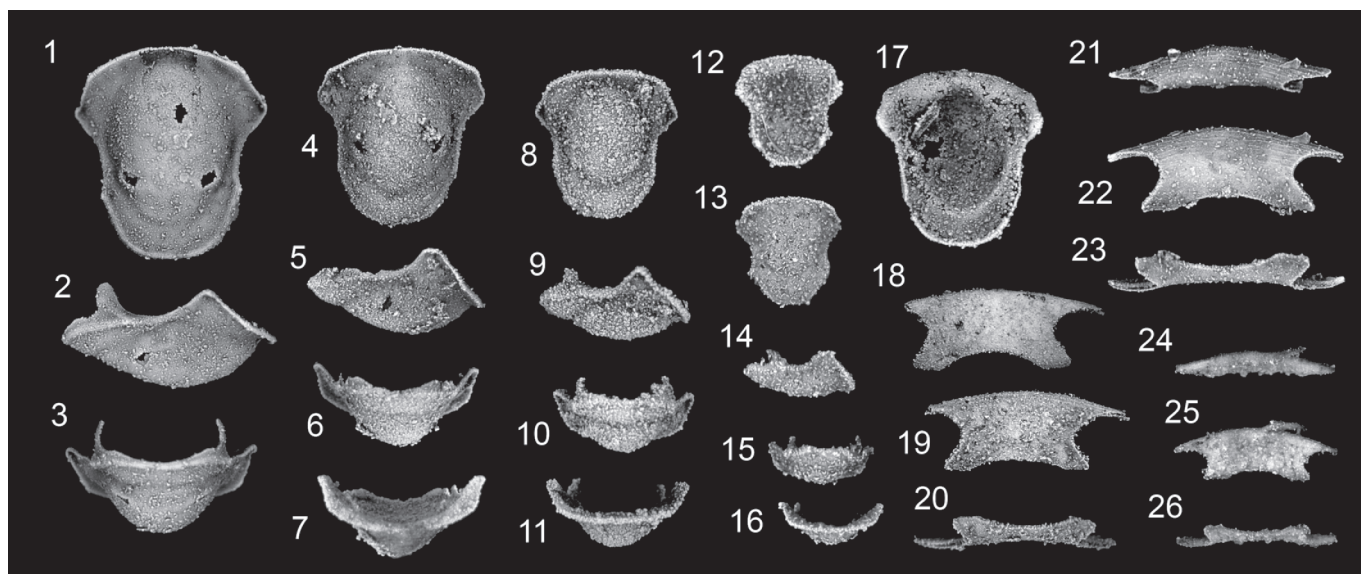


FIGURE 7.—Silicified hypostomes and rostral plates of *Zacanthopsis palmeri* n. sp., morphologically mature except where indicated. 1–3, hypostome with prominent maculae and posterior wings, ventral, lateral, and posterior views, FMNH PE58187, $\times 10$; 4–7, 17, hypostome with maculae but missing posterior wings, ventral, lateral, posterior, anterior, and dorsal views, FMNH PE58161, $\times 10$; 8–11, hypostome, ventral, lateral, posterior, and anterior views, FMNH PE58188, $\times 10$; 12–16, hypostome, possibly morphologically immature, dorsal, ventral, lateral, posterior, and anterior views, FMNH PE58162, $\times 15$; 18, rostral plate, ventral view, FMNH PE58189, $\times 12$; 19, 20, rostral plate, ventral and posterior views, FMNH PE58165, $\times 12$; 21–23, rostral plate, anterior, ventral, and posterior views, FMNH PE58164, $\times 15$; 24–26, rostral plate, possibly morphologically immature, anterior, ventral, and posterior views, FMNH PE58215, $\times 15$. 1–3, 8–11, 18 from Klondike Gap, 4–7, 12–17, 19–23 from Ruin Wash, and 24–26 from Antelope Canyon.

In addition, the visual surface was strongly curved (Fig. 2.14, 2.18, 2.27), indicating a large field of view in the horizontal plane.

ONTOGENY

Ontogenetic description of *Zacanthopsis palmeri* n. sp. is based on silicified material from all localities (except One Wheel Canyon). Plotting cranial length against width (or the length and width of the entire dorsal shield for protaspides) does not separate protaspides from meraspides nor reveal discrete instars during any developmental period (Fig. 9). We divide the protaspid period into two stages based on differences in morphology. Two articulated specimens allow us to describe meraspis degree 1 (M1) and meraspis degree 3 (M3). Based on the size and morphology of the cranidia and pygidia in these specimens, other ontogenetic stages are described.

Early protaspis.—Figure 10.1–4. Dorsal exoskeleton subcircular in outline, moderately arched transversely and longitudinally. Glabella not defined. Closely spaced posterior fixigenal spines along the posterior margin. Posterior margin indented to superficially resemble a pygidial median notch. Thickened ventral margin between posterior fixigenal spines is

precursor to protopygidium of late protaspis. Hypostome almost the length of the dorsal sclerite (Fig. 10.2–3), anterior wings as large as middle body, extending laterally from narrow middle body, either merged with or serving as the rostral plate; lateralmost pair of spines on posterior border as long as anterior wings, extend postero-laterally; three additional pairs of spines on posterior border, shorter than lateralmost pair, extend dorsally (towards ventral side of dorsal sclerite).

Late protaspis.—Figure 10.5–10.10. Dorsal exoskeleton subcircular in outline; moderately arched transversely and longitudinally. Narrow glabella extends across dorsal sclerite, widens at LA. Four transverse glabellar furrows extend across glabella. Frontal pits separate the axial furrows from nearly complete marginal border. Protopygidium curved ventrally between reduced posterior fixigenal spines. Hypostome as in early protaspis with moderately well defined, posteriorly tapering middle body (Fig. 10.7).

MO(?)—M1.—Figure 10.21–23. Cranidium semicircular in outline. Glabella narrow, strongly expands anteriorly opposite anterior end of palpebral lobe, meets the anterior border. Anterior border curves smoothly to palpebral lobes. Palpebral lobe as narrow as anterior border, distinct from anterior border. Ocular ridge not defined. Posterior border furrow

←

FIGURE 6.—Morphologically mature thoracic segments and pygidia of *Zacanthopsis palmeri* n. sp. 1, 8, 18, 24, thoracic segment with very shallow curvature at fulcrum, dorsal, posterior, lateral, and anterior views, FMNH PE58190 $\times 7$; 2, 9, 17, 23, thoracic segment with moderately shallow curvature at fulcrum, dorsal, posterior, lateral, and anterior views, FMNH PE58191, $\times 7$; 3, 11, 15, 21, thoracic segment with moderately strong curvature at fulcrum, dorsal, posterior, lateral, and anterior views, FMNH PE58166, $\times 12$; 4, 12, 14, 20, thoracic segment with very strong curvature at fulcrum, dorsal, posterior, lateral, and anterior views, FMNH PE58192, $\times 7$; 5, 13, 19, thoracic segment with macroaxial spine and very strong curvature at fulcrum, dorsal, lateral, and anterior views, FMNH PE58167, $\times 10$; 6, 7, thoracic segment with macroaxial spine and very strong curvature at fulcrum, dorsal and lateral views, FMNH PE58193 $\times 9$; 10, 16, 22, thoracic segment with moderately strong curvature at fulcrum, posterior, lateral, and anterior views, FMNH PE58194, $\times 10$; 25–29, pygidium, dorsal, ventral, anterior, posterior, and lateral views, FMNH PE58168, $\times 10$; 30–34, pygidium, dorsal, ventral, anterior, posterior, and lateral views, FMNH PE58169, $\times 12$; 35–39, pygidium, dorsal, ventral, anterior, posterior, and lateral views, FMNH PE58170, $\times 15$; 40, pygidium, dorsal view, FMNH PE58199, $\times 15$; 41, pygidium, dorsal view, FMNH PE58171, $\times 20$; 42–46, pygidium, dorsal, ventral, anterior, posterior, and lateral views, FMNH PE58195, $\times 10$; 47, pygidium, dorsal view, FMNH PE58196, $\times 12$; 48, 49, pygidium, dorsal and lateral views, FMNH PE58197, $\times 10$; 50, 51, pygidium, dorsal and lateral views, FMNH PE58198, $\times 10$. 3, 5, 11, 13, 15, 19, 21, 25–39, 41 from Ruin Wash and 1, 2, 4, 6–10, 12, 14, 16–18, 20, 22–24, 40, 42–51 from Klondike Gap.

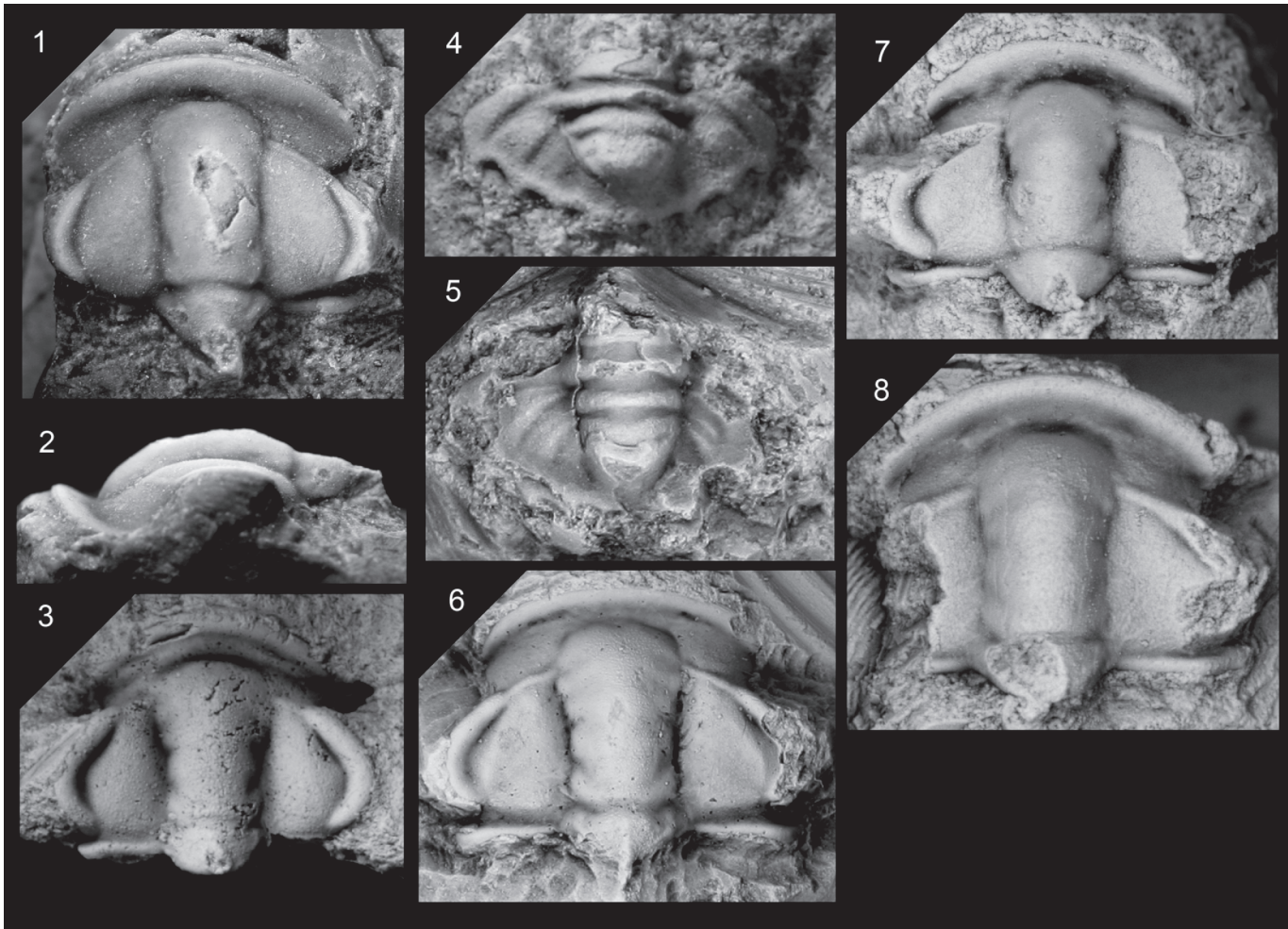


FIGURE 8—Specimens of other species of *Zacanthopsis*. 1, 2, *Zacanthopsis levis*, cranium, dorsal and lateral views, from the Pioche district (Lincoln County, Nevada), USNM 15445 (holotype), $\times 8$. 3, *Zacanthopsis contractus*, cranium, dorsal view, from the Saline Valley Formation (near Gold Point, Esmeralda County, Nevada), USNM 144287 (holotype), $\times 11$; 4, *Zacanthopsis levis*, pygidium, dorsal view, from the Saline Valley Formation (near Gold Point, Esmeralda County, Nevada), USNM 144286, $\times 15$; 5, *Zacanthopsis expansa*, pygidium, dorsal view, from the Illytd Formation (Wernecke Mountains, Yukon Territory, Canada), GSC 91829, $\times 8$; 6, *Zacanthopsis contractus* (formerly *Z. stribuccus*), cranium, dorsal view, from the Sekwi Formation (Mackenzie Mountains, Northwest Territories, Canada), GSC 27416, $\times 7$; 7, *Zacanthopsis expansa*, cranium, dorsal view, from the Illytd Formation (Wernecke Mountains, Yukon Territory, Canada), GSC 91776 (holotype), $\times 15$; 8, *Zacanthopsis expansa*, cranium, dorsal view, from the Illytd Formation (Wernecke Mountains, Yukon Territory, Canada), GSC 91777, $\times 15$.

straight, extends to lateral edge of cranium. Posterior border curves posteriorly to form fixigenal spine; fixigenal spine does not extend posterior of LO. LO triangular, tapers posteriorly into axial node.

M1.—Known from one incompletely preserved specimen which became partially disarticulated and broken during cleaning (FMNH PE58183–84, Fig. 10.11–16). Specimen approximately 0.5 mm in cephalic length. Cranium semicircular in outline. Glabella expands anteriorly. Hypostome fused to rostral plate; extends posteriorly halfway down cranial length, with laterally extending posterior spines, no longer than width (tr.) of middle body; denticulate posterior margin. One thoracic segment, slightly wider (tr.) than transitory pygidium, with axial spine. Transitory pygidium trapezoidal in outline. Two axial rings; axial spine on posterior ring. Two pairs of pleural spines extend from posterior margin; lateralmost oriented postero-dorsally; medialmost oriented postero-medially. See also Fig. 10.17–20.

Post-M1 transitory pygidium.—(Fig. 11.29–36). Description for M3 applies for all post-M1 transitory pygidia

M2 or *M3*.—Figure 11.1–22. Specimens of smaller size but similar cranial morphology as M3. Description of M3

applies with the following exceptions. Posterior border may curve posteriorly before curving antero-ventrally. Posterior wing extends laterally beyond palpebral lobe, curves ventrally at posterior end of palpebral lobe, ends bluntly (does not taper). Short, blunt posterior fixigenal spines occasionally present on postero-lateral end of posterior wing.

Fused rostral-hypostomal plate found disarticulated but associated with crania of this description (Fig. 11.21–22). Hypostome has well defined denticulate posterior margin, large middle body, tapering posteriorly, defined by posterior furrow. Rostral plate wide with blunt ends, strongly curved, extends laterally beyond hypostomal body, ornamentation of terrace lines.

M3.—One articulated enrolled specimen (FMNH PE58237, Fig. 11.23–28). Specimen is 1 mm in cephalic length, excluding occipital spine. Cranium trapezoidal. Glabella expands forward, meets anterior border. Dorsal glabellar surface flat (long.), curves strongly anteriorly at middle (sag.) of LA. S1–S4 unclear; SO straight, narrower than posterior border furrow. Posterior margin of LO curves posteriorly, dorsal surface upslowing posteriorly in lateral view (Fig. 11.26). Occipital spine as long as width (sag.) of LO, extends

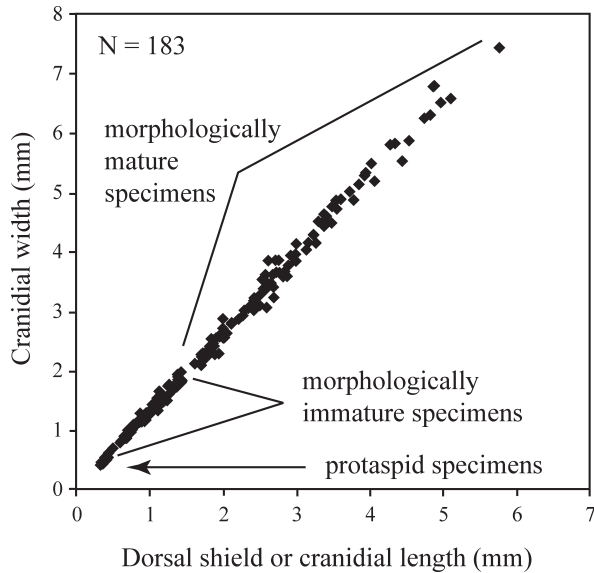


FIGURE 9—Cranial length-to-width ratio of specimens of *Zacanthopsis palmeri* n. sp. Cranial length includes the entire dorsal shield in protaspides and includes the occipital ring but excludes the occipital spine in all other specimens. Morphologically immature specimens includes obvious meraspides as well as those identified as immature based on the rate of overall shape change (see Fig. 13 and “Choice of specimens for analysis” under Geographic Variation).

posteriorly from dorsal surface of LO. Anterior border as wide (sag.) as palpebral lobes, of uniform width; merges smoothly with anteriorly convergent anterior branch of facial suture; subtle anterior arch. Palpebral lobes two thirds the length of the glabella, slightly curved, widest at lateralmost extent, tapering to anterior and posterior ends. Palpebral furrow

widest where palpebral lobe widest. Ocular ridge subparallel to anterior border, meets glabella at anterior end of LA. Very narrow frontal area anterior of ocular ridge. Interocular area arched transversely and longitudinally, summit higher than palpebral lobes but lower than dorsal surface of glabella. Posterior border straight, of similar width as axial furrow, extends to lateral edge of posterior wing. Posterior wing tapers laterally, extends laterally beyond palpebral lobes. Posterior border curves strongly posteriorly at fulcrum (Fig. 11.25).

Three thoracic segments, narrow, curve ventrally at fulcrum. Axial spines at least as long as occipital spine, curve posteriorly. Sentate pleural spines, posteriorly directed. Anteriormost thoracic segment narrower (tr.) than distance between tips of posterior wings.

Pygidium subquadrate in outline. Four axial rings with narrow axial spines curving postero-dorsally, anteriormost as long as width (tr.) of pygidium, decreasing in length down axis (Fig. 11.24, 26 show pygidial spines posterior to axial spine of posteriormost thoracic segment). Anteriormost spine as long as width of pleural field. Two to three pleural furrows visible; extend postero-laterally. Four pairs of pleural spines oriented posteriorly, decreasing in length medially, middle spines extend furthest posteriorly. See also Fig. 11.29–36.

Post-M3 cranidia.—Figure 11.37–40, 44–45. Specimens between 1 and 1.4 mm in cranial length, excluding occipital spine. Description of morphologically mature specimens applies with the following exceptions. Glabella subparallel or very gently expanding forward. Frontal area less strongly concave (curving upward) than in mature specimens; anterior arch more gently curving. Anterior border more strongly curved than in mature specimens but becomes less so in later meraspis. Preglabellar field as wide (sag.) as anterior border (sag.) but widens through later meraspis stages. Posterior

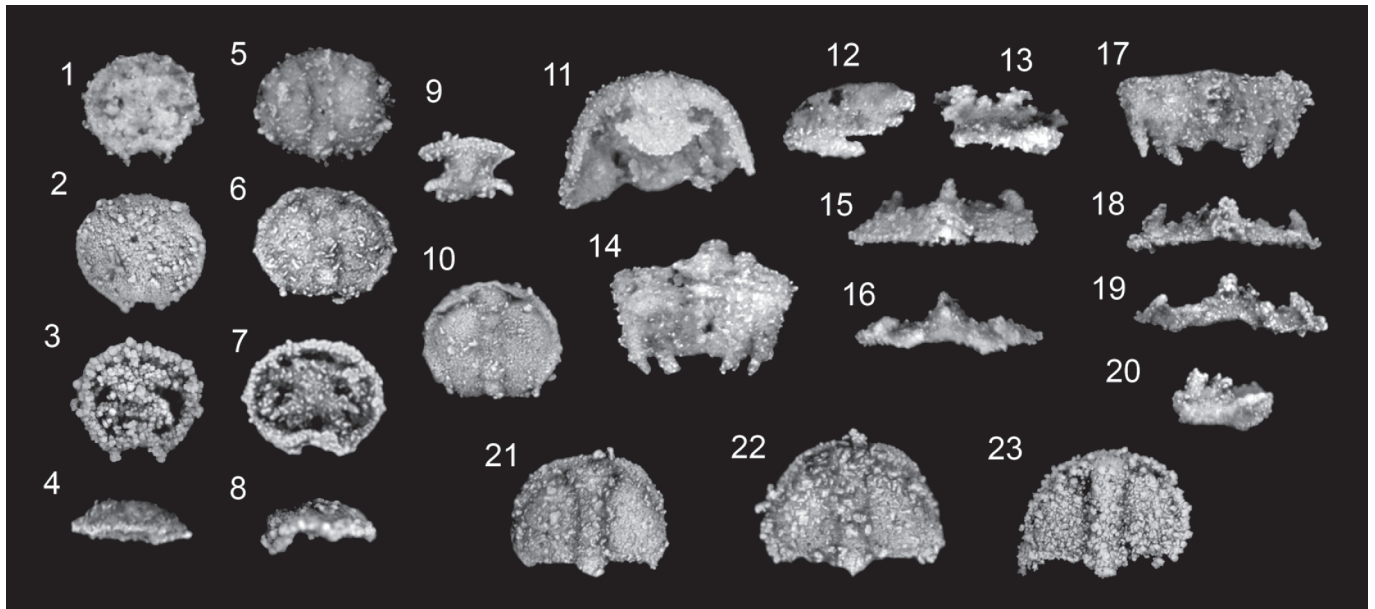
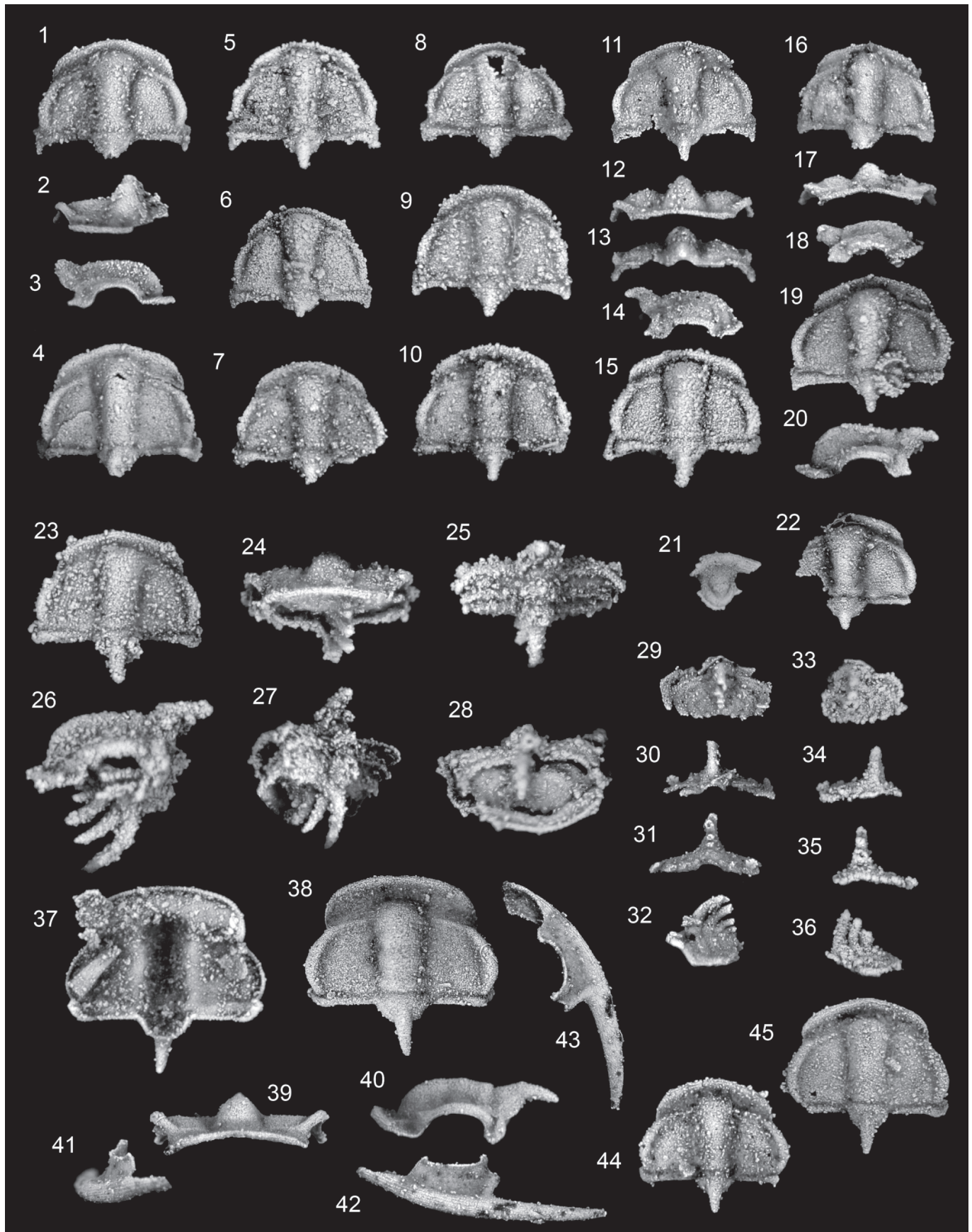


FIGURE 10—Silicified specimens representing the ontogenetic development of *Zacanthopsis palmeri* n. sp., protaspis and early meraspis stages. 1, early protaspis showing posterior fixiginal spines, dorsal view, FMNH PE58186, $\times 35$; 2, early protaspis showing posterior fixiginal spines, dorsal view, FMNH PE58212, $\times 35$; 3–4, early protaspis with hypostome, ventral and lateral views, FMNH PE58157, $\times 35$; 5, late protaspis, dorsal view, FMNH PE58185, $\times 35$; 6–8, late protaspis with hypostome, dorsal, ventral, and lateral views, FMNH PE58156, $\times 35$; 9, hypostome assigned to protaspis stage, ventral view, FMNH PE58163, $\times 35$; 10, Late protaspis showing four glabellar furrows, dorsal view, FMNH PE58155, $\times 35$; 11–12, cranidium with hypostome in meraspis degree 1, ventral and lateral views, FMNH PE58183, $\times 35$; 13–16, pygidium with thoracic segment in meraspis degree 1, lateral, dorsal, anterior, and posterior views, FMNH PE58184, $\times 35$; 17–20, pygidium likely in meraspis degree 1, dorsal, anterior, posterior, and lateral views, FMNH PE58173, $\times 35$; 21, cranidium likely in meraspis degree 0 or 1, dorsal view, FMNH PE58153, $\times 35$; 22, cranidium likely in meraspis degree 0 or 1, dorsal view, FMNH PE58154, $\times 35$; 23, cranidium likely in meraspis degree 0 or 1, dorsal view, FMNH PE58230, $\times 25$. 1, 5, 11–16 from Klondike Gap, 2 from Antelope Canyon, 3–4, 6–10, 17–22 from Ruin Wash, and 23 from Oak Springs Summit.



wings extend laterally just beyond palpebral lobes, taper laterally. Lateral end of posterior wing rounded. Posterior border gradually curves antero-ventrally at fulcrum.

Post-M3 librigena.—Figure 11.41–43. Description of morphologically mature librigena applies with the following exceptions. Ocular platform at least as wide as lateral border. Genal spine slightly shorter than pre-occipital cranial length.

Late meraspis hypostome.—Figure 7.12–16. Hypostome subovate, subovate anterior lobe. Anterior wings broad, triangular, extend dorso-laterally. Posterior wings narrower than anterior wings with bluntly rounded tips, extend directly dorsally; not visible in ventral view. Posterior body smaller than anterior lobe, low, defined by change in slope of hypostomal surface. Posterior margin more strongly rounded than hypostomal suture. Border narrow, well defined on anterior margin. No ornamentation.

Discussion.—Ontogenies previously described for corynexochine trilobites include *Paralbertella limbata* Rasetti, 1951 (described as *Albertella limbata* by Hu, 1985b), *Fieldaspis quadriangularis* Rasetti, 1951 (by Hu, 1985b), *Bathyriscus fimbriatus* Robison, 1964 (by Robison, 1967), *Ptarmigania aurita* Resser, 1939 (by Hu, 1971; Lee and Chatterton, 2003), *Glossopleura boccar* (Walcott, 1916) (by Hu, 1985a), *Corynexochides? expansus* Rasetti, 1967 (by Rasetti, 1967) and *Zacanthopsis levis* (by Smith, 1995).

The morphology of *Zacanthopsis palmeri* in the early protaspid period differs from that of Cambrian zacanthoidids *Fieldaspis quadriangularis* and *Paralbertella limbata* (Hu, 1985b), by lacking a frontal lobe or “axial knobs” and possessing distinct posterior fixigenal spines. In the later protaspid period, the posterior margin is indented and lacks the protruding terminal node seen in *F. quadriangularis* and *P. limbata*. In contrast, both early and late protaspid morphology of *Z. palmeri* is very similar to that of the Cambrian dolichometopids *Bathyriscus fimbriatus* (Robison, 1967) and *Ptarmigania aurita* (Hu, 1971; Lee and Chatterton, 2003). The protaspis is also similar to that of the co-occurring Ptychoparioid *Eokochaspis metalaspis* Sundberg and McColm, 2000 (ontogeny described by Palmer [1958] as *Crassifimbria walcotti* Resser, 1939), but the hypostome is markedly different. Both the anterior wings and the four pairs of spines on the posterior margin are shorter and blunter on *E. metalaspis*.

Throughout the meraspid period, the glabella becomes more parallel-sided, until it expands only slightly anteriorly. The frontal area expands anteriorly and laterally. The preglabellar field gets more concave (upward curving). The ocular ridge moves posteriorly from the anterior border; by the late meraspid period it is almost perpendicular to the sagittal axis. The palpebral lobes migrate laterally and the posterior wings migrate inward relative to the palpebral lobes. During earlier

meraspid degrees the posterior wing still carries the posterior fixigenal spine on the postero-lateral edge of the posterior wing. From M3, the posterior wing begins to taper distally and the fixigenal spine is lost. LO expands laterally and posteriorly to become even more strongly triangular. The occipital spine decreases in length relative to the length of the cranium. LO becomes less upsloping posteriorly with a smoother transition into the axial spine. It is not until later in the meraspid period that the anterior arch develops and the anterior branches of the facial sutures become divergent from the junction of the ocular ridge and palpebral lobe before curving adaxially towards the anterior border. The dorsal glabellar surface curves less strongly anteriorly. The posterior border begins to curve anteriorly as well as ventrally at the fulcrum. The junction between the ocular ridge and the glabella migrates posteriorly along LA. The interocular area becomes increasingly horizontal and sometimes upsloping abaxially. In the latest developmental stages, the palpebral lobes continue to migrate laterally and become more flexed.

The ocular platform of the librigena decreases in proportional width relative to the anterior border through ontogeny. The genal spine increases in length relative to cranial length.

The hypostome remains fused with the rostral plate through at least M3 (Fig. 11.21). Spines on the posterior margin decrease in size to denticles and are completely lost on all individuals with a functional hypostomal suture. In later stages of development, the anterior body of the hypostome becomes more bulbous and the furrow defining it becomes more distinct around the entire margin of the body but particularly on the posterior margin. The anterior margin is defined in earlier developmental stages; definition along the lateral and posterior margins increases as development progresses.

Stages of development in the transitory pygidium were insufficiently represented by specimens to recognize most instars. Nevertheless, post-M1 pygidia may be distinguished from M1 pygidia by an increase in the number of axial and pleural spines. Axial spines are not retained on the mature pygidium. Thus it appears that all axial spines occur on segments to be released into the thorax. The thoracic pleural spines in the thorax are much shorter than those on the pygidium.

GEOGRAPHIC VARIATION

The occurrence of six geographically distinct samples of comparable individuals from one silicified limestone bed provides an opportunity to test if all specimens belong to *Zacanthopsis palmeri* n. sp. and to assess the degree of morphological variation among any spatially segregated samples of this species.

←

FIGURE 11—Silicified specimens representing the ontogenetic development of *Zacanthopsis palmeri* n. sp. in later meraspis stages. 1–20, crania likely in M2 or M3: 1–3, dorsal, anterior, and lateral views, broken between photographs, FMNH PE58152, ×25; 4, dorsal view, FMNH PE58229, ×25; 5, dorsal view, FMNH PE58151, ×25; 6, dorsal view, FMNH PE58211, ×25; 7, dorsal view, FMNH PE58228, ×25; 8, dorsal view, FMNH PE58182, ×25; 9, dorsal view, FMNH PE58238, ×25; 10, dorsal view, FMNH PE58227, ×20; 11–14, dorsal, anterior, posterior, and lateral views, FMNH PE58239, ×25; 15, dorsal view, FMNH PE58181, ×20; 16–18, dorsal, anterior and lateral views, FMNH PE58209, ×25; 19–20, dorsal and lateral views, FMNH PE58210, ×25; 21, fused rostral-hypostomal plate likely in M2 or M3, ventral view, FMNH PE58208, ×25; 22, cranium associated with fused rostral-hypostomal plate in M2 or M3, broken posterior wing, dorsal view, FMNH PE58207, ×25; 23–28, partially enrolled articulated specimen, cranium in dorsal, anterior, posterior, and lateral views, oblique view, and pygidium in dorsal view, FMNH PE58237, ×25; 29–32, morphologically immature pygidium post-M1, dorsal, anterior, posterior, and lateral views, FMNH PE58200, ×25; 33–36, morphologically immature pygidium post-M1, dorsal, anterior, posterior, and lateral views, FMNH PE58172, ×25; 37–40, morphologically immature cranium post-M3, ventral, dorsal, anterior, and lateral views, FMNH PE58205, ×20; 41–43, morphologically immature librigena likely post-M3, anterior, lateral, and dorsal views, FMNH PE58214, ×20; 44, morphologically immature cranium post-M3, dorsal view, FMNH PE58180, ×20; 45, morphologically immature cranium post-M3, dorsal view, FMNH PE58205, ×20. 1–3, 5, 33–36 from Ruin Wash, 4, 7, 10 from Oak Springs Summit, 6, 16–22, 37–43, 45 from Antelope Canyon, 8, 15, 29–32, 44 from Klondike Gap, and 9, 11–14, 23–28 from Hidden Valley.

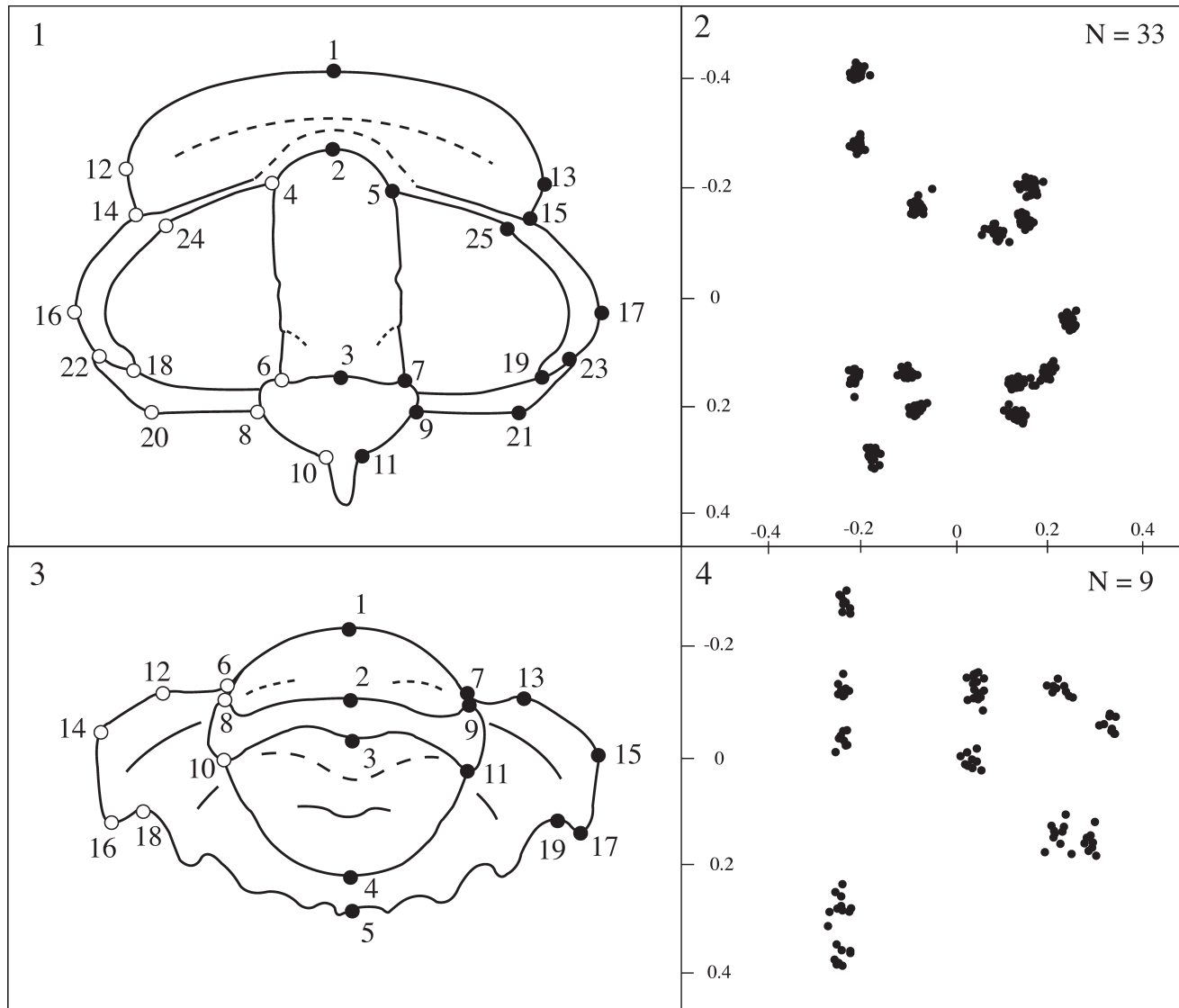


FIGURE 12—Diagrams showing chosen landmarks on cranium (1) and pygidium (3). See Appendix 1 for description of landmarks. All paired homologous landmarks are computationally reflected and averaged across the sagittal axis. Closed circles show configuration after averaging. Superimposition plot of cranial (2) and pygidial (4) specimens from Klondike Gap. The superimposition method shown is sliding baseline registration (see text).

Geometric morphometrics.—Morphological variation was assessed using geometric morphometric methods (Bookstein, 1991; Zelditch et al., 2004). Cranidia and pygidia were oriented for photography as described for systematic paleontology. Landmark coordinates (described below) were obtained from the photographs using ImageJ 1.36b (Rasband, 2006), freely available at <http://rsb.info.nih.gov/ij/>. Landmarks were digitized in dorsal view for both cranidia and pygidia.

Cranidium.—A total of 25 landmarks (three along the sagittal axis and 11 pairs on either side of the axis) were chosen that optimize summary of the overall shape of the cranium while retaining a reasonable sample size (Fig. 12.1, Appendix 1). Glabellar furrows were not consistently well defined across specimens of *Zacanthopsis palmeri* for use as landmarks.

Pygidium.—A total of 19 landmarks (five along the sagittal axis and seven pairs on either side of the axis) were chosen that optimize summary of the shape of the axial rings and the anteriormost pleural segments and spines, while retaining a reasonable sample size (Fig. 12.3, Appendix 1). The posterior

pleural spines were not preserved consistently enough for inclusion.

All paired landmarks were averaged across the sagittal axis because they cannot be regarded as independent (Zelditch et al., 2004; Zelditch, 2005). Averaging paired landmarks also allows for the inclusion of specimens where only one of the pair of landmarks is preserved. This reduces the total number of landmarks on the cranium to 14 and the total number of landmarks on the pygidium to 12.

All statistical analyses were performed using warp scores, which are derived from thin-plate spline decomposition (Rohlf, 1990; Bookstein, 1991; Zelditch et al., 2004). Variation within and between samples was visually compared using principal component analysis (PCA) of the warp scores. Canonical variates analysis of the warp scores and a bootstrapped *F*-test of Procrustes coordinates were used to test for significant differences between samples (Zelditch et al., 2004). We use a bootstrapped *F*-test because it does not assume an isotropic normal distribution of landmarks around

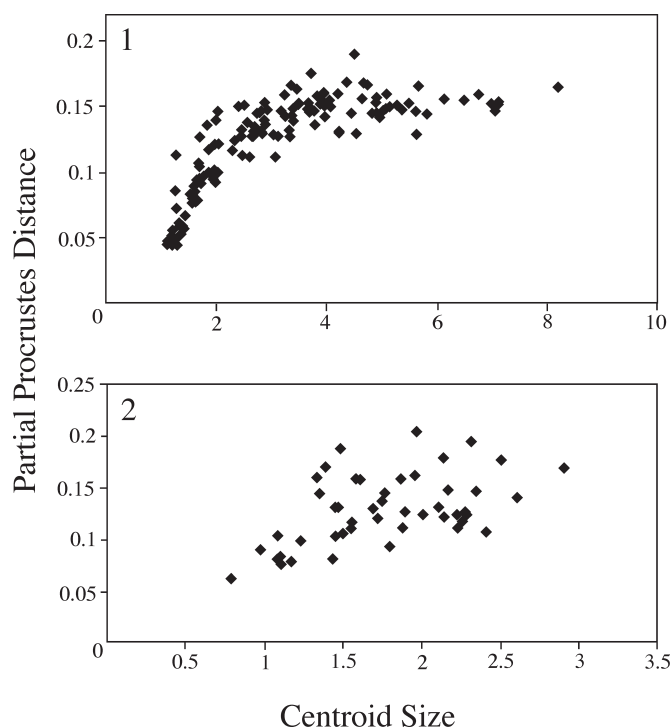


FIGURE 13—Partial Procrustes distance of each specimen from the mean configuration calculated from the three smallest specimens against centroid size (the square root of the sum of squared distances of all landmarks from their centroid). 1, Cranidia. Note that the partial Procrustes distance increases as centroid size increases until a centroid size of approximately 2, at which point partial Procrustes distance no longer increases at the same rate and instead varies around a partial Procrustes distance of 0.15. This break in slope is considered to be the centroid size at which mature morphology has been reached. A centroid size of 2.05 is equivalent to a cranium length of 1.4 mm. 2, Pygidia. Note absence of break in slope. Landmark configurations shown in Figure 12.

the mean; visual inspection of the variation around each landmark after Procrustes superimposition (e.g., Klondike Gap sample, Figure 12.2, 4) indicates that such an assumption is not met by these data. In order to compensate for the multiple comparisons made using the bootstrapped *F*-test, we applied a Bonferroni correction to the critical *p*-value. The degree of variation in each sample was measured as within-group variance in Procrustes distance away from the group mean. The

contribution to overall morphological variation by each sample was assessed using partial disparity (Foote, 1993). All analyses were performed using the Integrated Morphometrics Package (Sheets, 2003), freely available at <http://www3.canisius.edu/~sheets/morphsoft.html>.

Choice of specimens for analysis.—All cranidia with fixigenal spines were excluded from analysis because they lack landmarks which are clearly homologous to that defining the fulcrum in more mature specimens (landmarks 20 and 21, Fig. 12.1). In order to avoid inflating the apparent variation by including other morphologically immature specimens, the Procrustes distance of each of these specimens away from the mean configuration of the three remaining smallest specimens was plotted against the centroid size (Fig. 13.1). Generally, as the specimen size gets larger, the Procrustes distance also increases, indicating a progressive change in shape away from the juvenile reference form. At a centroid size of approximately 2, however, the slope of the Procrustes distance relative to size becomes less steep. Based on this change in slope, all specimens with centroid size greater than 2.05 were selected for analysis. Centroid size of 2.05 is equivalent to a sagittal cephalic length, including the occipital ring but excluding the occipital spine, of 1.4 mm.

Such a change in allometry has been documented for other trilobites and suggested to represent entry into the holaspide period, but there are cases where this change in allometry does not correspond with termination of trunk segment generation (Hughes and Chapman, 1995; Kim et al., 2002). Due to a paucity of articulated specimens, it is unknown whether this break in slope corresponds to entry into the holaspide period in *Zacanthopsis palmeri*, and this is considered unlikely given the small size of the specimens at this transition relative to the largest known specimens (cf. Hughes and Chapman, 1995). Here, this break in slope is used only to identify morphological maturity of the cranidia.

Pygidia were considered morphologically mature if they did not carry axial spines. Such specimens do show considerable allometric growth but no change in slope of Procrustes distance from the mean configuration of the smallest three specimens relative to specimen size (Fig. 13.2).

Sample sizes are shown in Table 1.

Removal of variation due to allometry. Of the morphologically mature specimens, there is no significant difference in size range of cranidia across localities (Fig. 14.1) but there is

TABLE 1—Within-sample variation and partial disparity of samples of *Zacanthopsis palmeri* based on shape data from both cranidia and pygidia. Variation and SE values are to 10³. SE = standard error, based on 1,600 bootstraps; %MD = percentage of morphological disparity that partial disparity represents. Samples are ordered from the northern- to southernmost localities.

	Non-size-standardized				Size-standardized		
	N	Variation	SE	%MD	Variation	SE	%MD
CRANIDIA							
RW	28	2.57	0.26	8.16	2.24	0.25	5.56
KG	33	2.05	0.25	8.16	1.86	0.19	5.56
AC	13	2.45	0.36	4.08	2.31	0.34	7.41
OS	6	1.98	0.37	20.41	1.66	0.34	22.22
HV	8	1.73	0.30	22.45	1.28	0.16	29.63
GS	2	2.05	1.02	36.73	NA	NA	29.63
same photo	20	0.34	0.06				
remountRW	20	0.19	0.03				
remountAC	20	0.19	0.02				
PYGIDIA							
RW	10	7.07	0.78	21.11	5.64	0.72	15.51
KG	9	4.92	0.93	11.56	4.50	0.84	20.86
AC	10	6.93	0.82	8.04	4.80	0.50	8.02
OS	7	8.54	1.31	44.22	6.66	1.17	35.83
HV	10	6.81	0.90	15.08	5.53	0.37	19.79
remountAC	20	0.40	0.11				

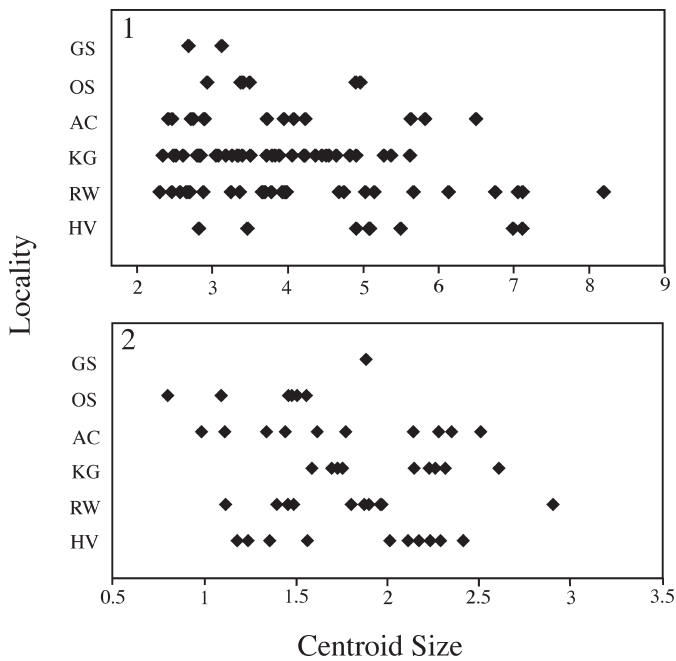


FIGURE 14—Range of centroid sizes of crania (1) and pygidia (2) for each locality. Locality abbreviations as in Figure 1.

some size sorting in pygidia across localities, particularly Oak Springs Summit and Klondike Gap (Fig. 14.2). Visual inspection of the partial warp and uniform warp scores against the natural log of the centroid size (\ln centroid size) indicated that shape changes linearly with size for all samples of crania and pygidia, even within morphologically mature subsamples (data not shown, but see Fig. 13). Because allometric shape change is linear, each specimen may be size-standardized based on the ontogenetic trajectory described by the sample. First, multiple regression of the partial and uniform warps against \ln centroid size is used to predict the shape of an individual at a certain size. The variation in the sample not due to allometry is preserved in the residuals from the regression. Thus the size-standardized shape for each specimen is that predicted by the regression plus its associated residuals (Zelditch et al., 2004; Kim et al., 2009). We used centroid size of 3.5 for crania and 1.5 for pygidia (\ln centroid size of 1.25 and 0.4, respectively) because all samples include specimens of these sizes (Fig. 14), but the regression and size-standardization was carried out separately for each sample. Specimens from Grassy Springs were not size-standardized because of extremely small sample size. Estimates of variation and results of bootstrapped F -test are reported for both size-standardized and non-size-standardized datasets.

With the exception of samples of crania from Klondike Gap and Antelope Canyon, size-standardization did not change the rank order of the estimates of within-sample variation or partial disparity for crania or pygidia. Results from PCAs of both the size-standardized and non-size-standardized data did not differ substantially in regards to the shape deformation or the percentage of variation described by each component.

Assessment of measurement error.—Orientation error was assessed by remounting and rephotographing the same specimen 20 times for two crania of different sizes (FMNH PE58141, cephalic length 4.86 mm (Fig. 2.3); FMNH PE58203, cephalic length 1.76 mm (Fig. 4.2) and one pygidium (FMNH PE58216, Fig. 4.14) and then digitizing

landmarks from each photograph. Digitizing error was assessed by extracting landmark coordinates from the same photograph of one specimen 20 times. Because the variances of the samples are an order of magnitude greater than the variance attributable to orientation or digitizing error for both crania and pygidia (Table 1), measurement error is deemed negligible.

Results: crania.—Figure 15 shows results from PCA of the size-standardized morphologically mature crania from the six samples. Data from error assessment are not included. PC 1 accounts for 17.0% of the total variation and relates primarily to the placement of the palpebral lobe and anterior branch of the facial suture relative to the rest of the cranium (Fig. 15.3). PC 2 accounts for 15.3% of the total variation and is related primarily to the width of the interocular area relative to the rest of the cranium and to the orientation of the palpebral lobe relative to the sagittal axis (Fig. 15.4). A smaller proportion of variation between specimens is due to differences in the location of the distal end of the posterior wing relative to the rest of cranium (e.g., PC 3, 9.2% of total variation). The shape of the glabella is fairly uniform across localities with the exception of minor differences in the length and width of the occipital ring. The length of the preglabellar field is uniform.

Two canonical variates are statistically significant discriminator of samples (Bartlett's test: Wilk's $\Lambda = 0.0693$, $\chi^2 = 197.5229$, d.f. = 120, $P < 0.001$; Wilk's $\Lambda = 0.1815$, $\chi^2 = 126.2863$, d.f. = 92, $P = 0.01$). While there is substantial overlap of samples in the PCA, the mean morphologies of a few samples remain significantly different from one another after the Bonferroni correction (bootstrapped F -test, Table 2). For example, there is a significant difference between means and minimal overlap in morphospace of samples from Hidden Valley and Oak Springs Summit (Fig. 15.1, 2). Though sample means are different, the mean morphology of the species is well represented by FMNH PE58174 (holotype) (Fig. 3.1) and FMNH PE58144 (Fig. 2.4). Morphological features characterizing specimens that lie on the outer edges of the occupied morphospace include either very weakly or very strongly divergent anterior sutures (e.g., compare Fig. 3.4 with Fig. 2.28) and very small or very large width to length ratio in the cranium (e.g., compare Fig. 2.30 with Fig. 2.31 and Fig. 5.16). Samples represented by a larger sample size show greater within-sample variation (Klondike Gap and Ruin Wash, Table 1, Fig. 15.1).

Results: pygidia.—Figure 16 shows results from PCA of size-standardized morphologically mature pygidia from the six samples. Data from error assessment was not included. Like crania, a few sample means remain significantly different from one another after Bonferroni correction (bootstrapped F -test, Table 2). There is more geographical separation along PC 1 in samples of pygidia than crania, though the extent to which all pygidial samples overlap increases after size-standardization. Samples of pygidia from Klondike Gap and Oak Springs Summit are no longer separated from one another by PC 1 but Oak Springs Summit is separated from the rest of the samples by PC 3 (Fig. 16.2). Nonetheless, specimens from Oak Springs Summit, Hidden Valley, and Grassy Springs tend to have lower PC 1 values and specimens from Klondike Gap, Ruin Wash, and Antelope Canyon tend to have higher PC 1 values suggesting morphological divergence between samples from the Chief Range and samples from the Delamar Mountains (Fig. 1). Two canonical variates are statistically significant discriminators of samples (Bartlett's test: Wilk's $\Lambda = 0.0178$, $\chi^2 = 130.9938$, d.f. = 80, P

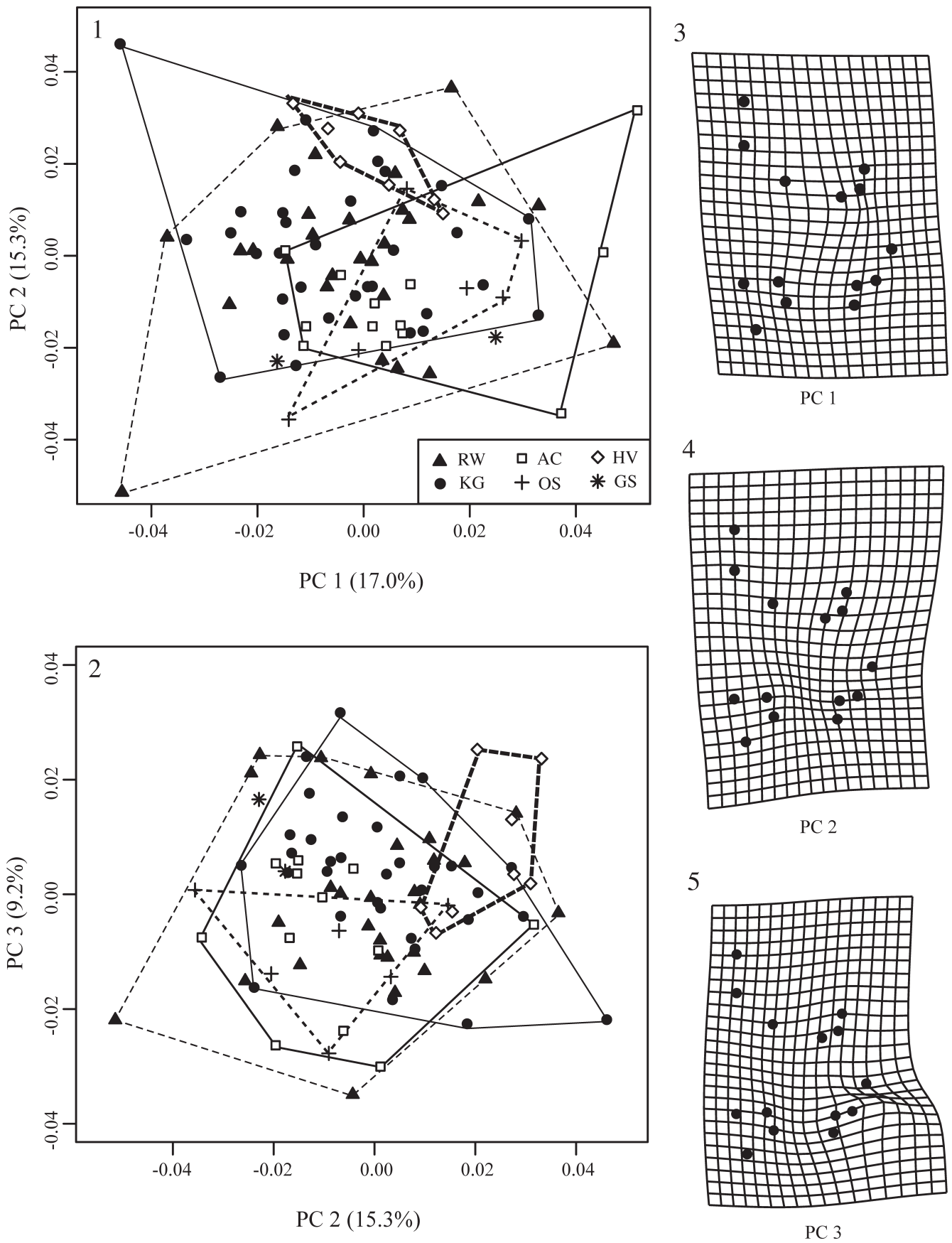


FIGURE 15—Principal components analysis (PCA) of *Zacanthopsis palmeri* mature crania after size standardization and not including error analyses. Percent variation summarized by each axis shown in axis label. 1, PC 1 vs. 2. 2, PC 2 vs. 3; locality abbreviations as in 15.1. 3, Thin-plate spline projections of variation along PC 1. 4, Thin-plate spline projection of variation along PC 2. 5, Thin-plate spline projection of variation along PC 3. See Figure 12 for landmark configuration. Locality abbreviations as in Figure 1.

TABLE 2—Pairwise comparisons of *Zacanthopsis palmeri* samples based on shape data from cranidia and pygidia. F = bootstrapped F -score based on 1,600 bootstraps of non-size standardized data; F^s = bootstrapped F -score based on 1,600 bootstraps of size-standardized data. P -values significant at $\alpha = 0.05$ in bold; P -values significant after Bonferroni correction in italics.

	CRANIDIA				PYGIDIA			
	F	P	F^s	P^s	F	P	F^s	P^s
KG vs RW	2.17	0.016	1.83	0.0531	1.38	0.2225	2.67	0.039
KG vs AC	2.19	0.024	2.43	0.012	0.45	0.8681	0.99	0.4181
KG vs HV	2.01	0.046	2.6	0.013	2.54	0.024	3.57	0.004
KG vs OS	2.72	0.012	2.77	0.008	4.3	0.006	4.13	0.005
RW vs AC	1.56	0.115	1.85	0.0544	0.96	0.4269	1.47	0.1813
RW vs HV	1.53	0.1338	2.53	0.011	3.13	0.008	3.79	0.007
RW vs OS	1.62	0.1069	1.92	0.0575	4.82	0.007	4.48	0.006
AC vs HV	1.96	0.047	3.59	0.004	2.24	0.049	2.98	0.016
AC vs OS	0.74	0.6475	0.93	0.4694	3.32	0.0138	3.58	0.008
HV vs OS	2.48	0.038	4.95	0.003	1.86	0.0875	2.51	0.023

< 0.001; Wilk's $\Lambda = 0.0944$, $\chi^2 = 76.6912$, d.f. = 57, $P = 0.04$).

Morphological variation across PC 1–3 is primarily expressed in the size of the pleural field relative to the axial lobe (Fig. 16.3–5). We note, however, that the shape of the variation within the remounted specimen is elliptical along PC 1. The resulting artificial inflation of variation along PC 1 is due to inconsistent orientation of the specimen with the articulating furrow vertical (recognized *a posteriori*). The magnitude of this error along this axis is not great enough, however, to account for all of the variation in the species along this axis. In addition, measurement error cannot explain the separation of geographic samples in morphospace.

With the exception of Oak Springs Summit, samples with greater sample sizes show greater variation. However, morphologically peripheral samples contribute more to species-level variation in pygidia than does sample size (Table 1). The sample from Oak Springs Summit has both high variation and contributes strongly to species-level variation. This is reflected in the PCA (Fig. 16.2): Oak Springs Summit occupies space along PC 3 that no other sample shares.

DISCUSSION

Cranidial shape change during ontogeny in *Zacanthopsis palmeri* n. sp. is dominated by lengthening of the ocular ridge, inward movement of the posterior wings, expansion of the preglabellar field, postero-lateral expansion of the occipital ring, widening of the interocular area, and transition from convergent anterior branches of the facial suture to divergent anterior branches (Fig. 17.1). In morphologically mature specimens, intraspecific variation is expressed in the same features, particularly the angle of divergence in the anterior branch of the facial suture and the width of the interocular area. Pygidial shape change during ontogeny is dominated by a decrease in the size of the pleural field relative to the axial lobe, decrease in the medial width of the anterior axial ring, and transition from a subtrapezoidal shape to subtriangular shape (Fig. 17.2). Again, intraspecific variation in morphologically mature specimens is expressed in the same features. While there is some change in the shape of the glabella and the pygidial axis, variation of morphologically mature specimens within the species is expressed predominantly in the pleural lobes of both sclerites.

No one sample encompasses all of the variation that is expressed by *Zacanthopsis palmeri* and the mean morphology at maturity of many samples is significantly different from others (Table 2). If we had only sampled from two localities with significantly different means and minimal overlap (e.g., samples of cranidia from Hidden Valley and Antelope Canyon

or samples of pygidia from Klondike Gap and Oak Springs Summit), we would have concluded that those samples represented different groups diagnosable by a unique range of continuous characters. However, after sampling from more localities and aggregating samples by successive pooling of samples that cannot be distinguished from one another (following Davis and Nixon, 1992), we find that these samples are not distinct from another. For example, while Antelope Canyon is significantly different from Hidden Valley, neither is significantly different from Ruin Wash.

Without the Bonferroni correction, a case could be made to distinguish Oak Springs Summit and Hidden Valley pygidia from Ruin Wash, Klondike Gap, and Antelope Canyon pygidia (Table 2). Because of the substantial overlap of samples in morphospace, however, we do not believe that these results warrant the erection of new species or subspecies. Any specimen falling within areas of overlap could not be diagnosed as a member of a particular group or sample without knowledge of the geographic location of the specimen. Thus, the best interpretation of these data is that the specimens represent one species with some morphological variation between pygidia from the Chief Range and pygidia from the Delamar Mountains (Fig. 1).

Interestingly, there is an inconsistency in the localities which show significant differences in mean pygidial form and those that show differences in mean cranidial form (Table 2). For example, while cranidia from Oak Springs Summit and Hidden Valley do not overlap along PC 2 or PC 3 (Fig. 15.1, 2), pygidia from these two localities are more closely aligned morphologically, particularly along PC 1 (Fig. 16.1). While we cannot know how many individuals contributed to these samples of molts nor if the cranidia were shed by the same individuals as the pygidia, the inconsistency between the distributions of variation in the two sclerites suggests a decoupling of the intrinsic controls on variation in different sclerites.

Unfortunately, environmental differences between localities that might be associated with geographic variation in *Zacanthopsis palmeri* are not readily apparent. The bed itself does not show obvious sedimentological differences between localities. While water depth was increasing at these localities during the late Dyeran (Webster, 2007b), the relative difference in water depth between localities when this bed was deposited is unknown. Further, the relative position of each locality to shoreline remains unclear. There is, however, a dramatic shift in the faunal assemblage between localities. Palmer (1998, fig. 3) recognized a *Zacanthopsis-Eokochoaspis* biofacies in uppermost Dyeran sediments at Log Cabin Mine and One Wheel Canyon (Fig. 18.1). Yet the relative abun-

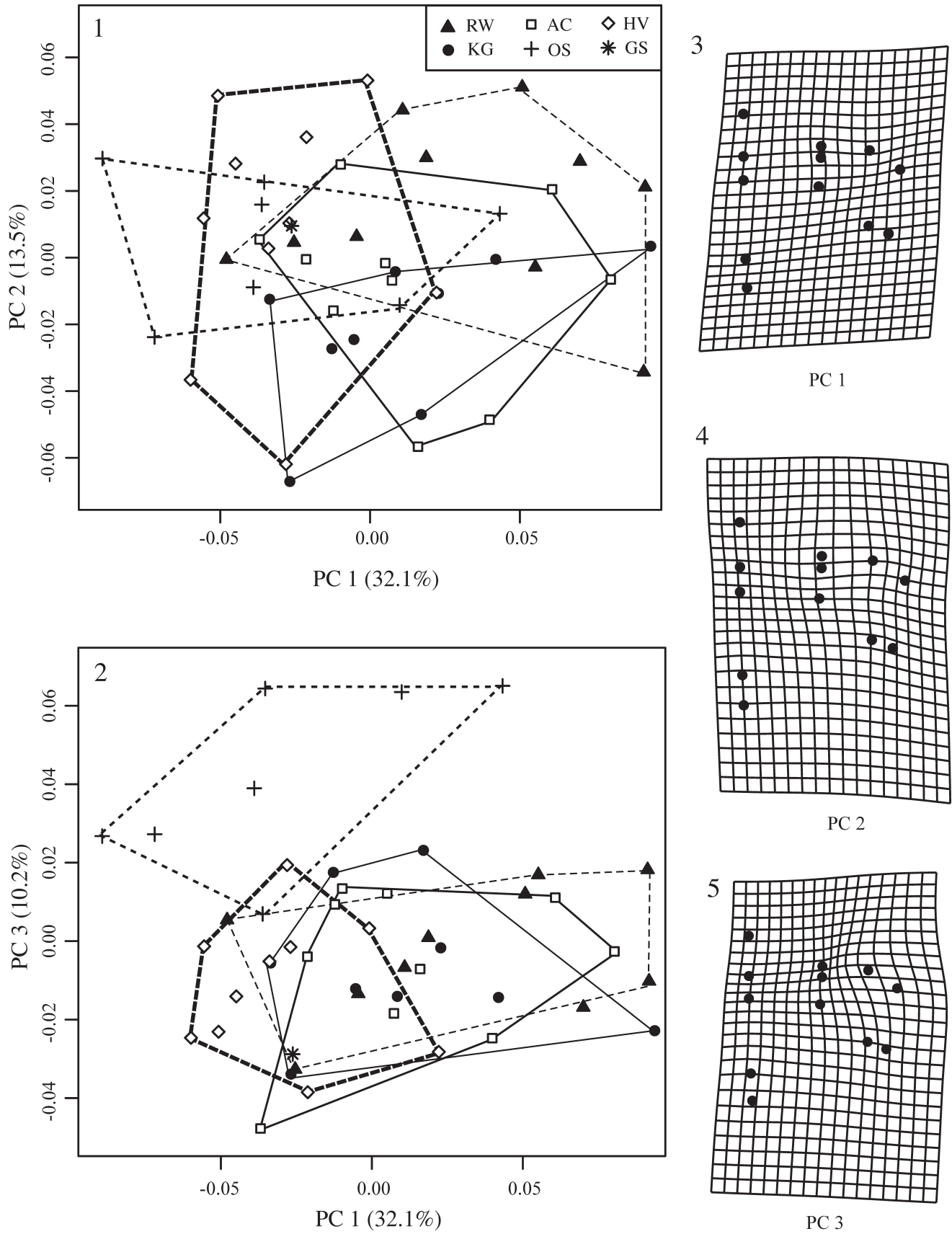


FIGURE 16—Principal components analysis (PCA) of *Zcanthopsis palmeri* mature pygidia after size standardization and not including error analyses. Percent variation summarized by each axis shown in axis label. 1, PC 1 vs. 2. 2, PC 1 vs. 3. 3, Thin-plate spline projection of variation along PC 1. 4, Thin-plate spline projection of variation along PC 2. 5, Thin-plate spline projection of variation along PC 3. See Figure 12 for landmark configuration. Locality abbreviations as in Figure 1.

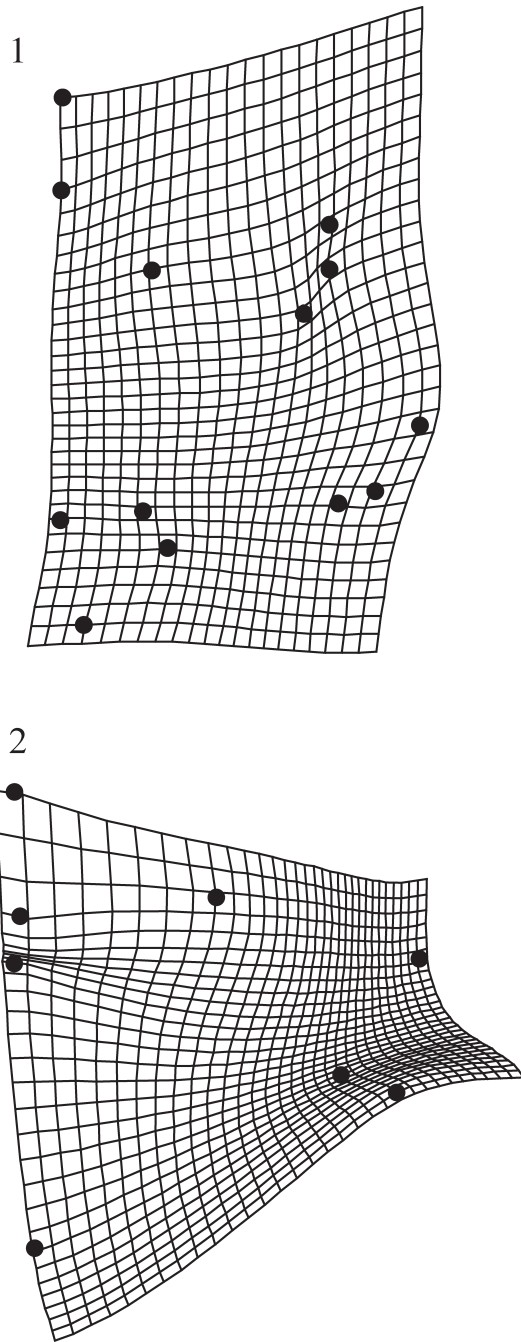


FIGURE 17—Thin-plate spline deformation plots showing morphological change through ontogeny. 1, Morphological change in cranium, based on same landmarks as shown in Figure 12.1 except landmarks 20–21 (total landmarks = 13). Reference form is FMNH PE58152, (cephalic length = 0.86 mm, Fig. 11.1) and target form is FMNH PE58201 (cephalic length = 4.04 mm, Fig. 4.4). 2, Morphological change in pygidium, based on landmarks 1–3, 5–7, and 14–19 shown in Figure 12.3 (total landmarks in analysis = 8). Reference form is FMNH PE58173 (pygidial length = 0.24 mm, Fig. 10.17) and the target form is FMNH PE58216 (pygidial length = 1.54 mm, Fig. 4.14).

dance of *Z. palmeri* changes so much across its geographic range that a sample from Grassy Springs better represents Palmer's *Olenellus-Nephrolenellus* biofacies (Fig. 18.3, Palmer [1998, fig. 3]) in regards to relative abundance. At Ruin Wash and Klondike Gap, *Z. palmeri* dominates the sample (Fig. 18.2). Such dramatic variation in relative abundance

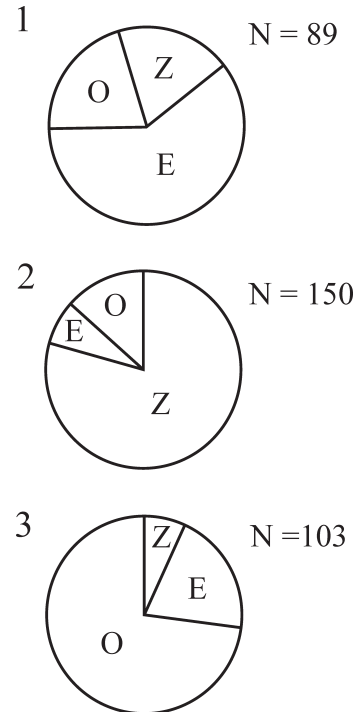


FIGURE 18—Relative abundances of trilobites at three sites; material from Klondike Gap (2) and Grassy Spring (3) are from the same bed. Counts were made of cranidia larger than 1 mm in cranial width. Z = *Zacanthopsis palmeri*; E = *Eokochoaspis metalaspis*, and O = olenelloid trilobites (including *Nephrolenellus*, *Olenellus*, and/or *Bolbolenellus*). Charts in order from northernmost locality to southernmost locality. 1, Log Cabin Mine/One Wheel Canyon, data from Palmer (1998, fig. 3). 2, Klondike Gap section, data from UCR 10097. 3, Grassy Spring section, data from ICS-10252.

suggests that some so far undetectable environmental difference existed between localities.

Comparison to previously described Zacanthopsis species.—Most species of *Zacanthopsis* are represented by one or only a few cranidia preserved in limestone, and, for some species, pygidia are unknown (Fig. 8). PCA of *Zacanthopsis* specimens shows that the cranidium of *Z. palmeri* is distinct from those of previously described species (Fig. 19, see Appendix 2 for list of specimens included in this analysis). Size standardization of *Z. palmeri* species did not alter the results of the PCA. The difference in shape between many of the species, however, is no greater than the range of variation within *Z. palmeri*, highlighting the need for large sample sizes for robust species delimitation. Indeed, the recognition of the morphological variation in other *Zacanthopsis* species based on new material from Greenland has recently motivated workers to synonymize species originally defined on the basis of one or two specimens (Blaker and Peel, 1997). Discrete characters, such as consistency in width of ocular ridge or numbers of axial furrows on the pygidia, and comparison of ontogenetic trajectories of shape change (such as that of *Z. levis* relative to *Z. palmeri*, to be published elsewhere) help to distinguish some *Zacanthopsis* species. Others remain most readily recognized by relative shape proportions, such as degree of anterior expansion of the glabella, length of the ocular ridge, or the width of palpebral lobes relative to frontal area, the latter of which also shows intraspecific variation among similar-sized specimens.

While the mean morphologies of some samples of *Zacanthopsis palmeri* are significantly different from one

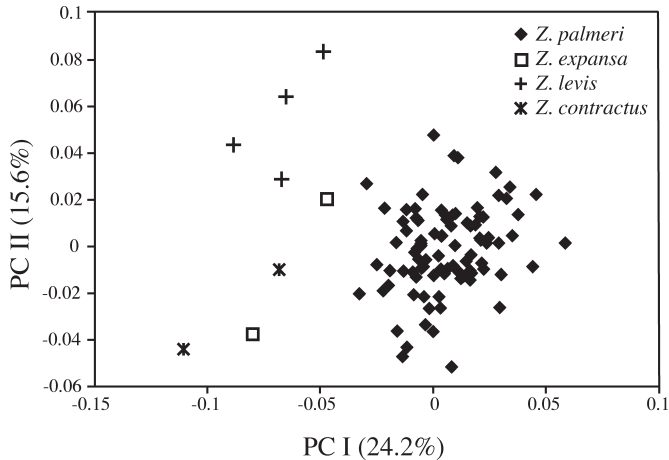


FIGURE 19—Principal components analysis (PCA) of cranidia of *Zacanthopsis* species. All morphologically mature *Z. palmeri* cranidia are included but are not size-standardized. See Appendix 2 for list of specimens of congeneric species. Landmark configuration shown in Figure 12.

another, within-sample variation accounts for most of the variation in the species (Fig. 15, 16). Moreover, there is no unique combination of characters that distinguish one sample from another, nor are there unique combinations of characters that distinguish clusters of specimens within samples. This, in addition to ontogenetic and discrete morphological characters separating *Z. palmeri* from other *Zacanthopsis* species, indicates that these samples belong to the same species but that this species expressed considerable within- and among-sample variation.

SUMMARY

Assessing geographic variation in the fossil record requires accounting for allometric growth, taphonomy, and time-averaging between localities, as well as measurement error for quantitative traits. Despite apparent sedimentological homogeneity across localities where *Zacanthopsis palmeri* n. sp. is found, no single sample encompasses all of the variation expressed by this species. In addition, different exoskeletal components have different patterns of variation. While the degree of intraspecific shape variation in *Z. palmeri* is as great as the shape difference between congeneric species, *Z. palmeri* is distinguishable from other species based on overall shape, discrete morphological features, and ontogeny. While variation exists within and among samples of *Z. palmeri*, samples cannot be consistently distinguished from one another by a unique combination of characters. Finally, the shift between the fused rostral-hypostomal plate and a functional hypostomal suture during *Zacanthopsis* ontogeny has not been reported from any other corynexochine taxa. Instead, corynexochines are generally characterized by a fused rostral-hypostomal plate throughout ontogeny (Fortey, 1990; Chatterton and Speyer, 1997). Because the nature of hypostomal attachment is relevant to order-level systematics and phylogenetics within Trilobita, this characteristic of *Zacanthopsis* may have bearing on corynexochid affinities, particularly in the relationship between this order and other early Cambrian taxa.

ACKNOWLEDGMENTS

We thank M. Foote, D. Jablonski, M. LaBarbara, and E. Sperling for helpful comments and discussion and assistance in the field. J. Paterson and an anonymous reviewer provided constructive reviews. J. Dougherty and R. Fontaine (Geological

Society of Canada), J. Thompson (Smithsonian), and S. Butts and C. McClintock (Yale Peabody Museum) kindly provided specimens of other species of *Zacanthopsis*. R. McKenzie assisted in picking specimens from insoluble residues.

REFERENCES

- ADRAIN, J. M. AND S. R. WESTROP. 2005. Late Cambrian ptychaspide trilobites from western Utah: implications for trilobite systematics and biostratigraphy. *Geological Magazine*, 142:377–398.
- ADRAIN, J. M. AND S. R. WESTROP. 2006. *Notchpeakia*, a new genus of Upper Cambrian (Sunwaptan) “entomaspidid” trilobites. *Journal of Paleontology*, 80:1152–1171.
- AVISE, J. C. 2000. *Phylogeography*. Harvard University Press, Cambridge, Massachusetts, 447 p.
- BEST, R. V. 1961. Intraspecific variation in *Encrinurus ornatus*. *Journal of Paleontology*, 35:1029–1040.
- BLAKER, M. R. AND J. S. PEEL. 1997. Lower Cambrian trilobites from North Greenland. *Meddelelser om Grønland, Geoscience*, Vol. 35, 145 p.
- BOOKSTEIN, F. L. 1991. *Morphometric Tools for Landmark Data: Geometry and Biology*. Cambridge University Press, Cambridge, 435 p.
- CHATTERTON, B. D. E. AND S. E. SPEYER. 1997. Ontogeny, p. 173–247. In R. L. Kaesler (ed.), *Treatise on Invertebrate Paleontology*. Pt. O. Arthropoda 1, Trilobita, Revised, 1. Geological Society of America and University of Kansas Lawrence Press, Lawrence.
- CISNE, J. L., G. O. CHANDLEE, B. D. RABE, AND J. A. COHEN. 1980a. Geographic variation and episodic evolution in an Ordovician trilobite. *Science*, 209:925–927.
- CISNE, J. L., G. O. CHANDLEE, B. D. RABE, AND J. A. COHEN. 1982. Clinal variation, episodic evolution, and possible parapatric speciation: the trilobite *Flexicalymene senaria* along an Ordovician depth gradient. *Lethaia*, 15:325–341.
- CISNE, J. L., J. MOLENOCK, AND B. D. RABE. 1980b. Evolution in a cline: the trilobite *Triarthrus* along an Ordovician depth gradient. *Lethaia*, 13:47–59.
- DAVIS, J. I. AND K. C. NIXON. 1992. Populations, genetic variation, and the delimitation of phylogenetic species. *Systematic Biology*, 43:421–435.
- EDDY, J. D. AND L. B. MCCOLLUM. 1998. Early Middle Cambrian *Albertella* biozone trilobites of the Pioche Shale, southeastern Nevada. *Journal of Paleontology*, 72:864–887.
- FOOTE, M. 1993. Contributions of individual taxa to overall morphological disparity. *Paleobiology*, 19:403–419.
- FORTEY, R. A. 1990. Ontogeny, hypostome attachment, and trilobite classification. *Palaeontology*, 33:529–576.
- FRANCE, S. C. 1993. Geographic variation among three isolated populations of the hadal amphipod *Hirondelella gigas* (Crustacea: Amphipoda: Lysianassoidea). *Marine Ecology Progress Series*, 92:277–287.
- FRITZ, W. H. 1972. Lower Cambrian trilobites from the Sekwi Formation type section, Mackenzie Mountains, Northwestern Canada. *Geological Survey of Canada Bulletin* 212, 58 p.
- FRITZ, W. H. 1991. Lower Cambrian trilobites from the Illtyd Formation, Wernecke Mountains, Yukon Territory. *Geological Survey of Canada Bulletin* 409, 77 p.
- HU, C.-H. 1971. Ontogeny and sexual dimorphism of Lower Paleozoic Trilobita. *Palaeontographica Americana*, 7:31–155.
- HU, C.-H. 1985a. Ontogenetic development of Cambrian trilobites from British Columbia and Alberta, Canada (Pt. I). *Journal of the Taiwan Museum*, 38:121–158.
- HU, C.-H. 1985b. Ontogenies of two middle Cambrian corynexochid trilobites from the Canadian Rocky Mountains. *Transactions and Proceedings of the Palaeontological Society of Japan*, new series, 138:138–147.
- HUGHES, N. C. 1991. Morphological plasticity and genetic flexibility in a Cambrian trilobite. *Geology*, 19:913–916.
- HUGHES, N. C. 1993. Distribution, taphonomy, and functional morphology of the Upper Cambrian trilobite *Dikelocephalus*. *Milwaukee Public Museum Contributions in Biology and Geology* 84, 49 p.
- HUGHES, N. C. 1994. Ontogeny, intraspecific variation, and systematics of the Late Cambrian trilobite *Dikelocephalus*. *Smithsonian Contributions to Paleobiology* 79, 89 p.
- HUGHES, N. C., AND R. E. CHAPMAN. 1995. Growth and variation in the Silurian trilobite *Aulacopleura konincki* and its implications for trilobite palaeobiology. *Lethaia*, 28:333–353.
- HUNDA, B. R., N. C. HUGHES, AND K. W. FLESSA. 2006. Trilobite taphonomy and temporal resolution in the Mt. Orab shale bed (Upper Ordovician, Ohio, U.S.A.). *Palaios*, 21:26–45.

- KIM, K., H. D. SHEETS, R. A. HANEY, AND C. E. MITCHELL. 2002. Morphometric analysis of ontogeny and allometry of the Middle Ordovician trilobite *Triarthrus becki*. *Paleobiology*, 28:364–377.
- KIM, K., H. D. SHEETS, AND C. E. MITCHELL. 2009. Geographic and stratigraphic change in the morphology of *Triarthrus becki* (Green) (Trilobita): A test of the *Plus ça change* model of evolution. *Lethaia*, 42:108–125.
- KOBAYASHI, T. 1935. The Cambro-Ordovician formations and faunas of South Chosen. *Palaeontology*. Part 3: Cambrian faunas of South Chosen with a special study on the Cambrian trilobite genera and families. *Journal of the Faculty of Science, Imperial University of Tokyo, Section II*, 4:49–344.
- LEE, D.-C. AND B. D. E. CHATTERTON. 2003. Protaspides of *Leiostiegium* and their implications for membership of the order Corynexochida. *Palaeontology*, 46:431–445.
- LIEBERMAN, B. S. 1998. Cladistic analysis of the Early Cambrian olenelloid trilobites. *Journal of Paleontology*, 72:59–78.
- MERRIAM, C. W. 1964. Cambrian rocks of the Pioche Mining District. U.S. Geological Survey Professional Paper 469, 59 p.
- NIXON, K. C. AND Q. D. WHEELER. 1990. An amplification of the phylogenetic species concept. *Cladistics*, 6:211–223.
- OWEN, D. D. 1852. Report of the Geological Survey of Wisconsin, Iowa, and Minnesota. Lippencott, Grambo and Co., Philadelphia, 638 p.
- PALMER, A. R. 1958. Morphology and ontogeny of a Lower Cambrian ptychoparioid trilobite from Nevada. *Journal of Paleontology*, 32:154–170.
- PALMER, A. R. 1964. An unusual Lower Cambrian trilobite fauna from Nevada. U.S. Geological Survey Professional Paper, 483-F, 13 p.
- PALMER, A. R. 1965. Trilobites of the Late Cambrian Pteroccephaliid biome in the Great Basin, United States. U.S. Geological Survey Professional Paper, 493, 105 p.
- PALMER, A. R. 1968. Cambrian trilobites of east-central Alaska. U.S. Geological Survey Professional Paper, 559-B, 115 p.
- PALMER, A. R. 1971. The Cambrian of the Great Basin and adjacent areas, western United States, p. 1–78. *In* C. H. Holland (ed.), *Cambrian of the New World*. Wiley-Interscience, New York.
- PALMER, A. R. 1998. Terminal Early Cambrian extinction of the Olenellina: Documentation from the Pioche Formation, Nevada. *Journal of Paleontology*, 72:650–672.
- PENG, S., L. E. BABCOCK, AND H. LIN. 2004. Polymerid trilobites from the Cambrian of Northwestern Hunan, China. Volume 1: Corynexochida, Lichida, and Asaphida. Science Press, Beijing, 333 p.
- RASBAND, W. S. 2006. ImageJ 1.36b. U.S. National Institutes of Health, Bethesda, Maryland.
- RASETTI, F. 1951. Middle Cambrian stratigraphy and faunas of the Canadian Rocky Mountains. *Smithsonian Miscellaneous Collections* 116, 277 p.
- RASETTI, F. 1967. Lower and Middle Cambrian trilobite faunas from the Taconic Sequence of New York. *Smithsonian Miscellaneous Collections* 152, 111 p.
- RESSER, C. E. 1938. Cambrian system (restricted) of the southern Appalachians. *Geological Society of America Special Papers* 15, 140 p.
- RESSER, C. E. 1939. The Ptarmigania strata of the northern Wasatch Mountains. *Smithsonian Miscellaneous Collections* 24, 72 p.
- RISKA, B. 1981. Morphological variation in the horseshoe crab *Limulus polyphemus*. *Evolution*, 35:647–658.
- ROBISON, R. A. 1964. Late Middle Cambrian faunas from western Utah. *Journal of Paleontology*, 38:510–566.
- ROBISON, R. A. 1967. Ontogeny of *Bathyriscus fimbriatus* and its bearing on affinities of corynexochid trilobites. *Journal of Paleontology*, 41:213–221.
- ROHLF, F. J. 1990. Rotational fit (Procrustes) methods, p. 227–236. *In* F. J. Rohlf and F. L. Bookstein (eds.), *Proceedings of the Michigan Morphometrics Workshop*, University of Michigan Special Publication 2.
- RUSHTON, A. W. A. AND N. C. HUGHES. 1996. Biometry, systematics, and biogeography of the late Cambrian trilobite *Maladioidella abdita*. *Transactions of the Royal Society of Edinburgh: Earth Sciences*, 87:1–10.
- SHAW, A. B. 1957. Quantitative trilobite studies II. Measurement of the dorsal shell of non-agnostidean trilobites. *Journal of Paleontology*, 31:193–207.
- SHEETS, H. D. 2003. *Integrated Morphometrics Package*. Canisius College, Buffalo, New York.
- SMITH, L. H. 1995. The role of species level phenotypic and developmental variability in the early evolution of animals. Unpublished Ph.D. dissertation, Harvard University, Cambridge, Massachusetts, 201 p.
- SMITH, L. H. 1998a. Asymmetry of Early Paleozoic trilobites. *Lethaia*, 31:99–112.
- SMITH, L. H. 1998b. Species level phenotypic variation in lower Paleozoic trilobites. *Paleobiology*, 24:17–36.
- SUNDBERG, F. A. 1999. Redescription of *Alokistocare subcoronatum* (Hall and Whitfield, 1877), the type species of *Alokistocare*, and the status of Alokistocaridae Resser, 1939B (Ptychopariida: Trilobita: Middle Cambrian). *Journal of Paleontology*, 73:1126–1143.
- SUNDBERG, F. A. 2004. Cladistic analysis of Early-Middle Cambrian kochaspid trilobites (Ptychopariida). *Journal of Paleontology*, 78:920–940.
- SUNDBERG, F. A. AND L. B. MCCOLLUM. 1997. Oryctocephalids (Corynexochida: Trilobita) of the Lower-Middle Cambrian boundary interval from California and Nevada. *Journal of Paleontology*, 71:1065–1090.
- SUNDBERG, F. A. AND L. B. MCCOLLUM. 2000. Ptychopariid trilobites of the Lower-Middle Cambrian boundary interval, Pioche Shale, southeastern Nevada. *Journal of Paleontology*, 74:604–630.
- SWINNERTON, H. H. 1915. Suggestions for a revised classification of trilobites. *Geological Magazine*, 6:487–496, 538–545.
- TAYLOR, M. E. AND R. B. HALLEY. 1974. Systematics, environment, and biogeography of some Late Cambrian and Early Ordovician trilobites from eastern New York State. U.S. Geological Survey Professional Paper 834, 38 p.
- WALCOTT, C. D. 1886. Second contribution to the studies on Cambrian faunas of North America. U.S. Geological Survey Bulletin 30, 369 p.
- WALCOTT, C. D. 1916. Cambrian Geology and Paleontology III. No. 5, Cambrian Trilobites. *Smithsonian Miscellaneous Collections*, 64:303–456.
- WALCOTT, C. D. 1924. Cambrian geology and paleontology V. No. 2, Cambrian and Ozarkian trilobites. *Smithsonian Miscellaneous Collections*, 75:53–60.
- WEBBER, A. J. AND B. R. HUNDA. 2007. Quantitatively comparing morphological trends to environment in the fossil record (Cincinnatian Series, Upper Ordovician). *Evolution*, 61:1455–1465.
- WEBSTER, M. 2003. Olenelloid trilobites of the southern Great Basin, U.S.A., and a refinement of uppermost Dyeran biostratigraphy. *Geological Society of America, Abstracts with Programs*, 35:166.
- WEBSTER, M. 2007a. Ontogeny and evolution of the Early Cambrian trilobite genus *Nephrolenellus* (Olenelloidea). *Journal of Paleontology*, 81:1168–1193.
- WEBSTER, M. 2007b. *Paranephrolenellus*, a new genus of Early Cambrian olenelloid trilobite. *Memoirs of the Association of Australasian Palaeontologists*, 34:31–59.
- WEBSTER, M., R. R. GAINES, AND N. C. HUGHES. 2008. Microstratigraphy, trilobite biostratigraphy, and depositional environment of the “Lower Cambrian” Ruin Wash Lagerstätte, Pioche Formation, Nevada. *Palaeogeography, Palaeoclimatology, Palaeoecology*, 264:100–122.
- WEBSTER, M. AND N. C. HUGHES. 1999. Compaction-related deformation in Cambrian olenelloid trilobites and its implications for fossil morphometry. *Journal of Paleontology*, 73:355–371.
- WEBSTER, M., H. D. SHEETS, AND N. C. HUGHES. 2001. Allometric patterning in trilobite ontogeny: testing for heterochrony in *Nephrolenellus*, p. 105–144. *In* M. L. Zelditch (ed.), *Beyond Heterochrony: the evolution of development*. Wiley-Liss, Inc., New York.
- WEBSTER, M. AND M. L. ZELDITCH. 2005. Evolutionary modifications of ontogeny: heterochrony and beyond. *Paleobiology*, 31:354–372.
- WESTROP, S. R. AND J. M. ADRAIN. 2007. *Bartonaspis* new genus, a trilobite species complex from the base of the Upper Cambrian Sunwaptan Stage in North America. *Canadian Journal of Earth Sciences*, 44:987–1003.
- WESTROP, S. R., R. LUDVIGSEN, AND C. H. KINDLE. 1996. Marjuman (Cambrian) agnostoid trilobites of the Cow Head Group, western Newfoundland. *Journal of Paleontology*, 70:804–829.
- WHEELER, Q. D. AND R. MEIER. 2000. *Species Concepts and Phylogenetic Theory*. Columbia University Press, New York, 230 p.
- WHITTINGTON, H. B. 1988. Hypostomes and ventral cephalic sutures in Cambrian trilobites. *Palaeontology*, 31:577–609.
- WHITTINGTON, H. B. 2009. The Corynexochina (Trilobita): a poorly understood suborder. *Journal of Paleontology*, 83:1–8.
- WHITTINGTON, H. B. AND S. R. A. KELLY. 1997. Morphological terms applied to Trilobita, p. 313–329. *In* R. L. Kaesler (ed.), *Treatise on Invertebrate Paleontology, Part O, Arthropoda 1, Trilobita, Revised, 1*. Geological Society of America and University of Kansas Press, Lawrence.
- ZELDITCH, M. L. 2005. Developmental regulation of variation, p. 249–276. *In* B. Hallgrímsson and B. K. Hall (eds.), *Variation: a central concept in biology*. Elsevier Academic Press, New York.
- ZELDITCH, M. L., D. L. SWIDERSKI, H. D. SHEETS, AND W. L. FINK. 2004. *Geometric Morphometrics for Biologists*. Elsevier Academic Press, New York, 443 p.

APPENDIX 1

Description of all landmarks shown in Figure 12.

Cranidial sagittal landmarks:

1—Intersection of the sagittal line and anterior margin of anterior border.

2—Intersection of the sagittal line and anterior margin of the glabella (or the preglabellar furrow).

3—Intersection of the sagittal line and the occipital furrow.

Cranidial paired landmarks:

4, 5—Intersection of the posterior margin of the ocular ridge and axial furrow.

6, 7—Junction of the axial furrow and occipital furrow at posterior margin of L1.

8, 9—Junction of posterior margin of posterior border and the posterior margin of LO.

10, 11—Junction of posterior margin of LO and the occipital spine.

12, 13—Angular junction of anterior facial suture with anterior margin of the anterior border. Coincident with the lateral-most extent of frontal area.

14, 15—Junction of anterior facial suture and palpebral lobe.

16, 17—Point of maximum curvature of lateral edge of palpebral lobe. Coincident with point of lateral-most extent of palpebral lobe.

18, 19—Junction of posterior end of palpebral lobe and posterior border furrow.

20, 21—Angular junction at fulcrum on posterior margin of posterior border.

22, 23—Junction of posterior limb and palpebral lobe.

24, 25—Junction of posterior margin of ocular ridge and anterior end of palpebral lobe.

Pygidial sagittal landmarks:

1—Intersection of sagittal line with anterior margin of articulating half ring.

2—Intersection of sagittal line with anterior edge of first axial ring.

3—Intersection of sagittal line with posterior edge of first axial ring.

4—Intersection of sagittal line and posterior edge of terminal axial piece.

5—Intersection of sagittal line and posterior margin.

Pygidial paired landmarks:

6, 7—Intersection of anterior margin of articulating half ring and anterior margin of the pleural field.

8, 9—Intersection of the anterior edge of the first axial ring and the axial furrow.

10, 11—Intersection of the posterior edge of the first axial ring and the axial furrow.

12, 13—Angular junction at fulcrum on anterior margin.

14, 15—Lateral edge of anterior margin of anterior segment.

16, 17—Distal tip of first pleural spine.

18, 19—Intersection of posterior side of base of first pleural spine and posterior margin.

APPENDIX 2

Below is a list of specimens (cranidia) of species other than *Zacanthopsis palmeri* included in the analysis in Figure 19. See Figure 8 for illustration of holotypes. USNM: U.S. National Museum (Smithsonian); GSC: Geological Society of Canada.

Zacanthopsis levis (Walcott, 1886): USNM 15445, holotype (from Pioche district, Lincoln County, Nevada). USNM 153535, 153537 (from Campbell Ranch section, Pioche Formation, White Pine County, Nevada). USNM 94756, formerly *Zacanthopsis virginica* Resser, 1938, holotype (from Shady Dolomite, near Austinville, Wythe County, Virginia). See Blaker and Peel (1997) for synonymy.

Zacanthopsis contractus Palmer, 1964: USNM 144287, holotype (from USGS Colln. 3748-CO, Saline Valley Formation, near Gold Point, Esmeralda County, Nevada). GSC 27416, formerly *Zacanthopsis sribuccus* Fritz, 1972, holotype (from GSC locality 73067, Sekwi Formation, Mackenzie Mountains, Northwest Territories, Canada). See Blaker and Peel (1997) for synonymy.

Zacanthopsis expansa Fritz, 1991: GSC 91776, holotype; GSC 91777, paratype (from GSC locality 90666, Illtyd Formation, Wernecke Mountains, Yukon Territory, Canada).